Geological Society of Zimbabwe Macgregor Memorial Lecture 2022

# Geological Evolution and Metallogeny of the Palaeoproterozoic Magondi Belt, Zimbabwe and Botswana

**Dr Sharad Master**
EGRI, School of Geosciences, University of the Witwatersrand, Johannesburg, South Africa. Sharad.master@wits.ac.za

# Part 2

Harare 21 October 2022
Bulawayo 24 October 2022

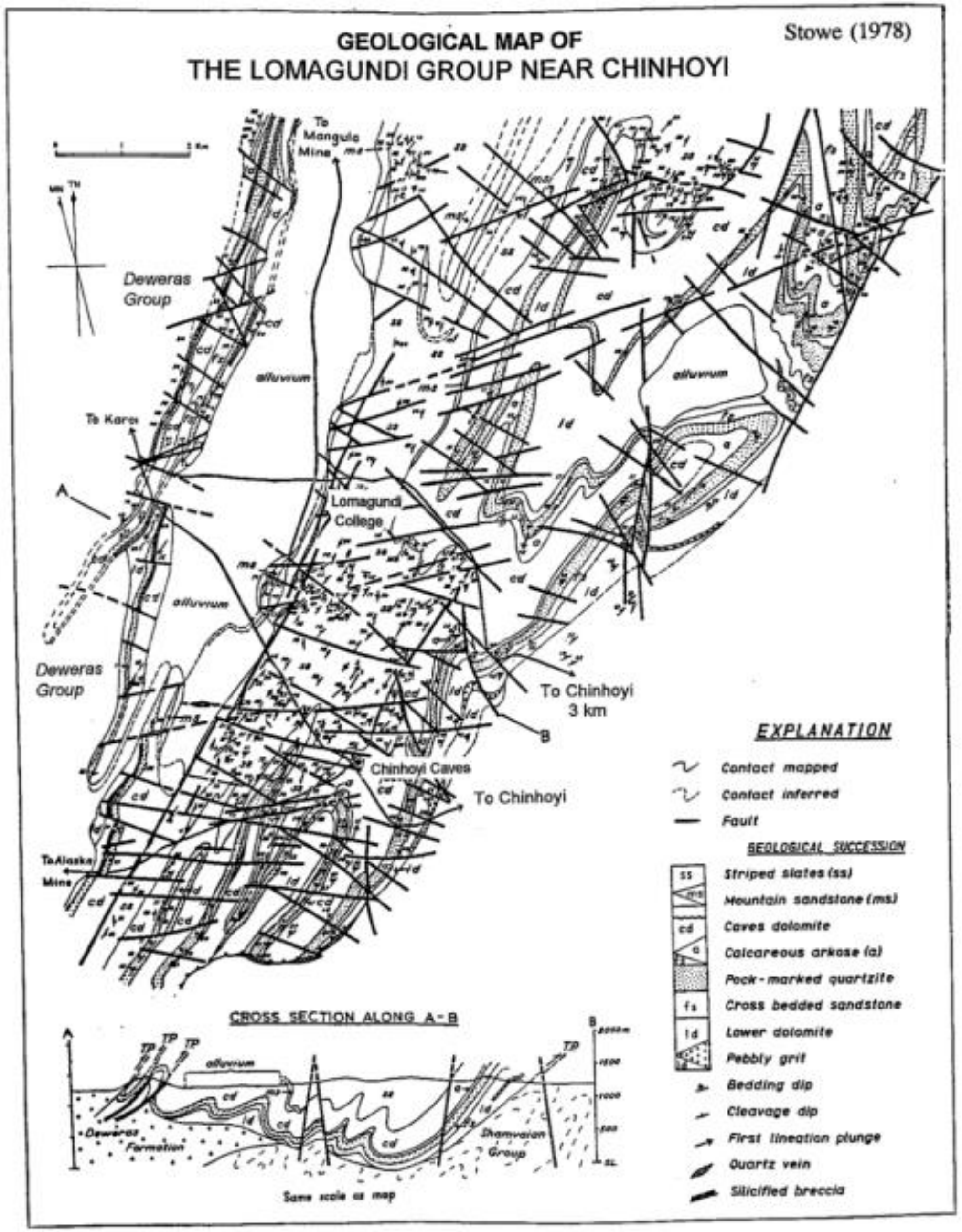


Geological Map of the Lomagundi Group near Chinhoyi (after Stowe, 1978)

# Lomagundi Group

# Lomagundi Group

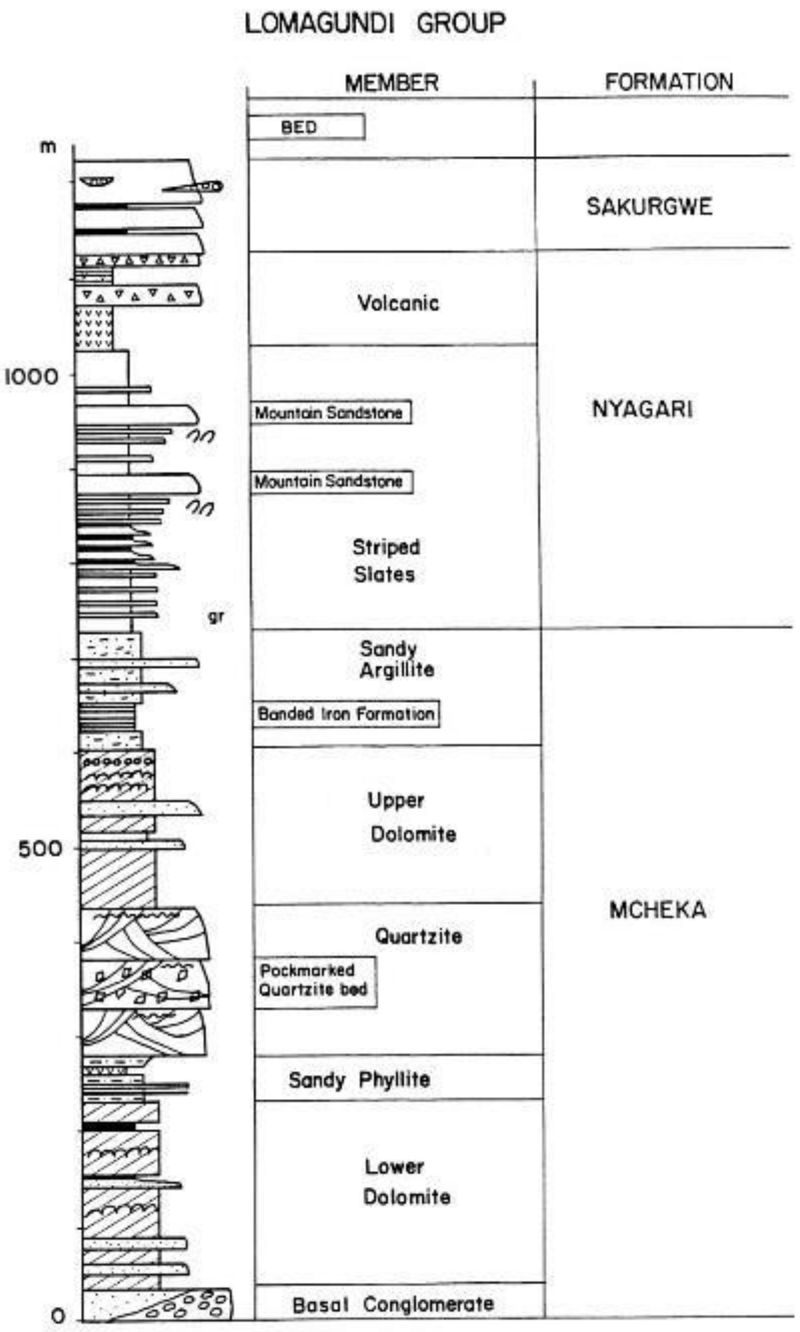


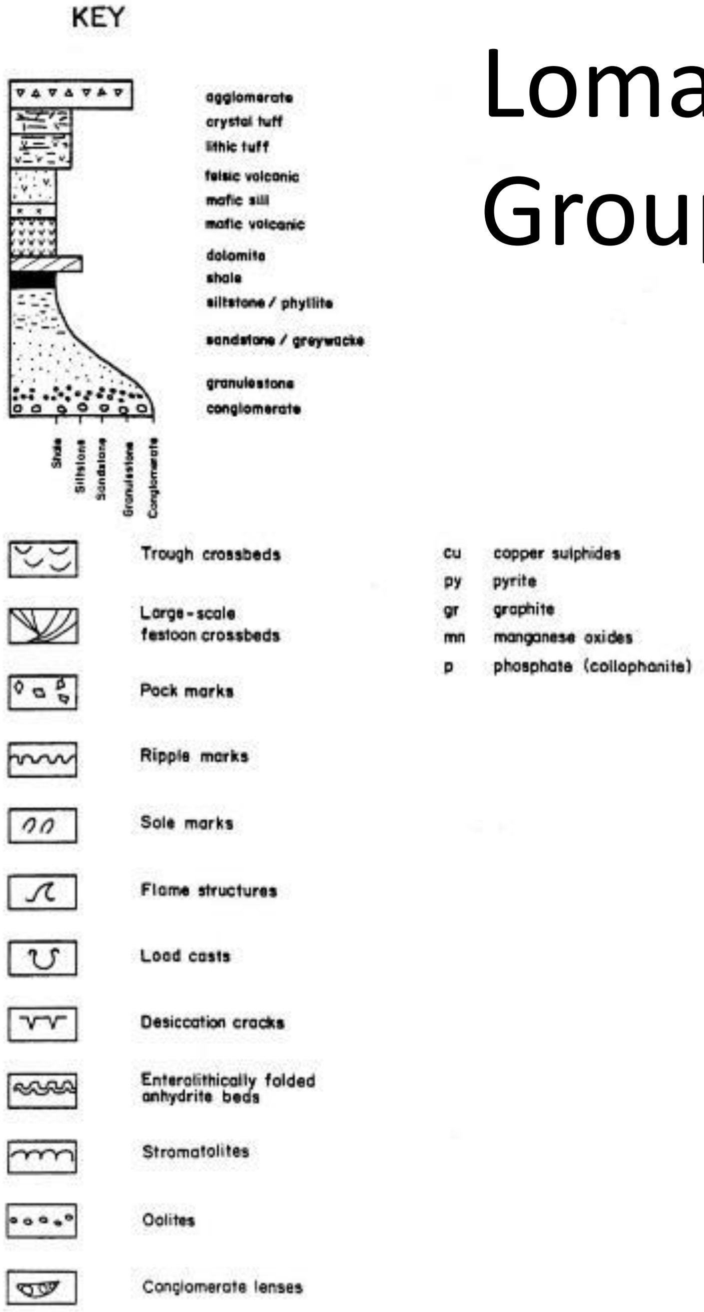

**Lomagundi Group**- post-rift sag basin carbonate platform

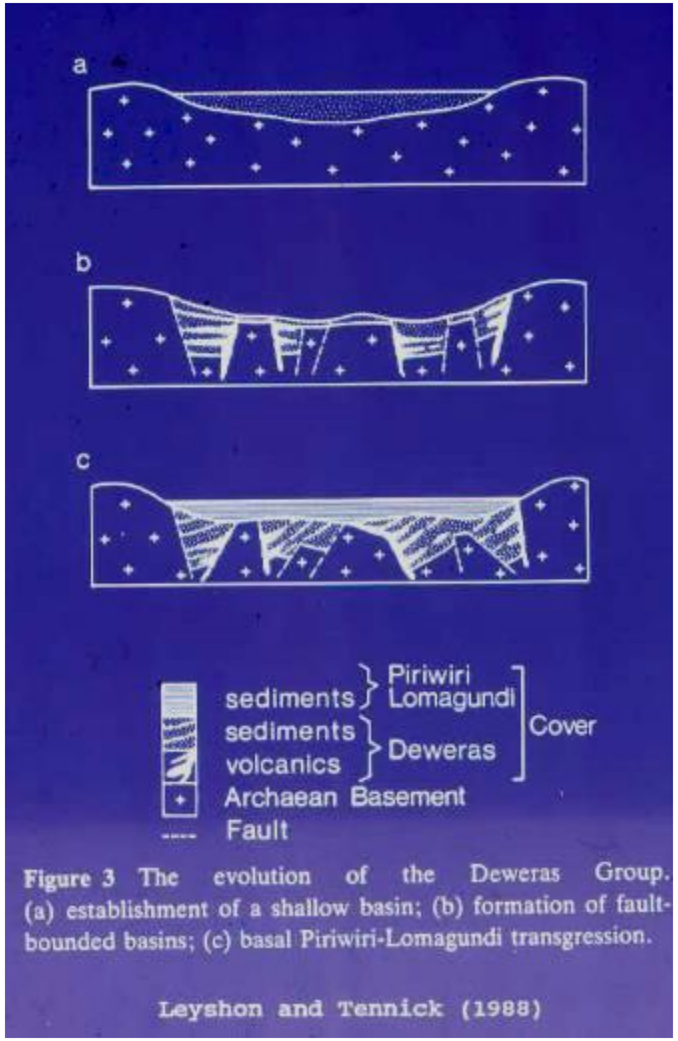


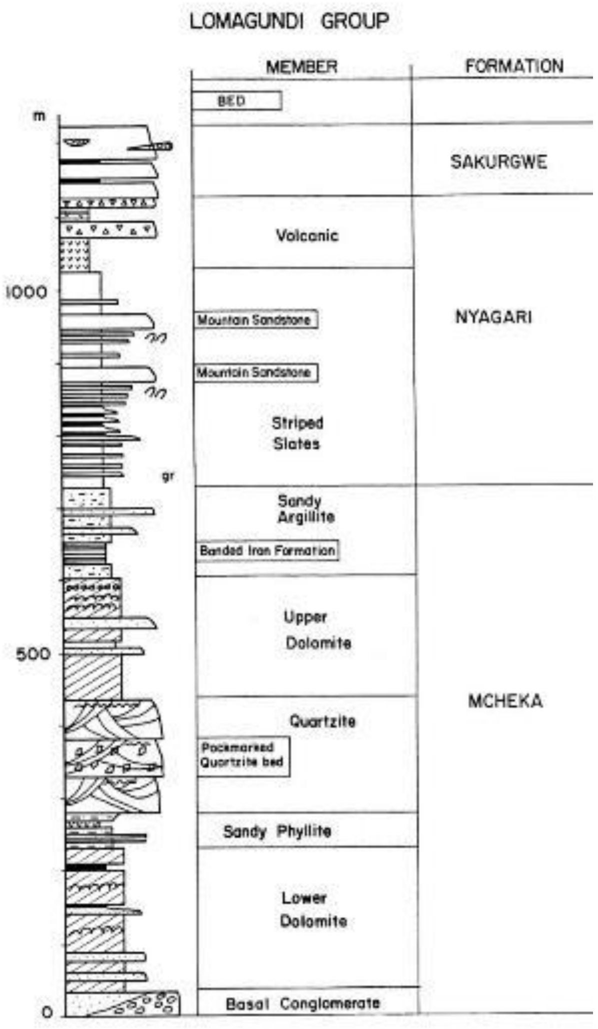


Lower Dolomite, Mcheka Formation, Lomagundi Group

Lower Dolomite, Mcheka Formation, Lomagundi Group

Upper Dolomite, Mcheka Formation, Lomagundi Group

Plan view of deformed domical stromatolites, Lower Dolomite, Lomagundi Group

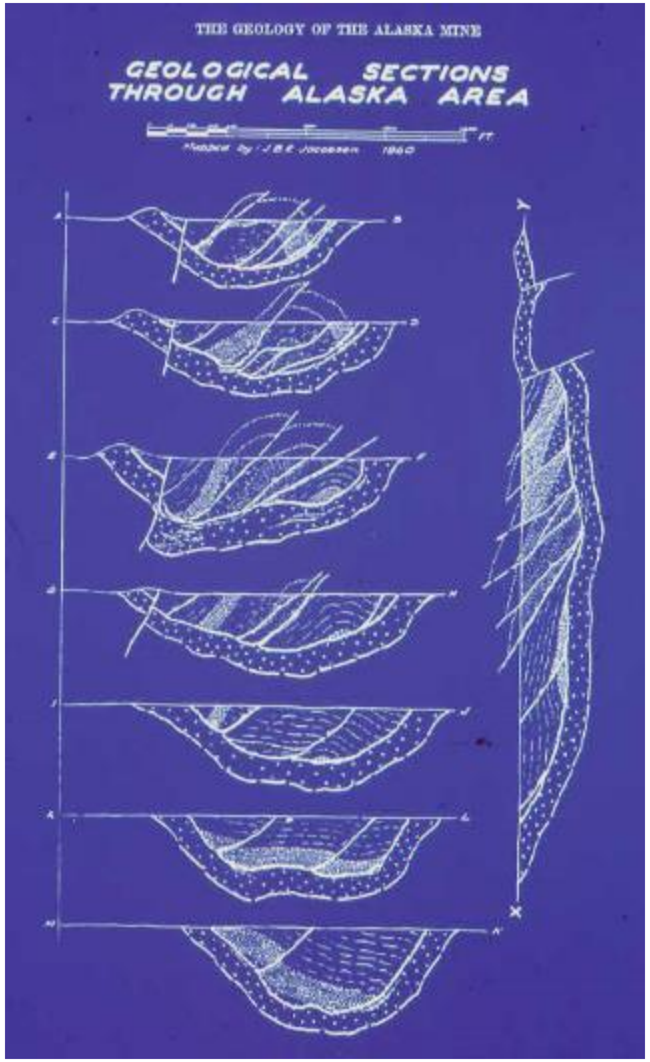


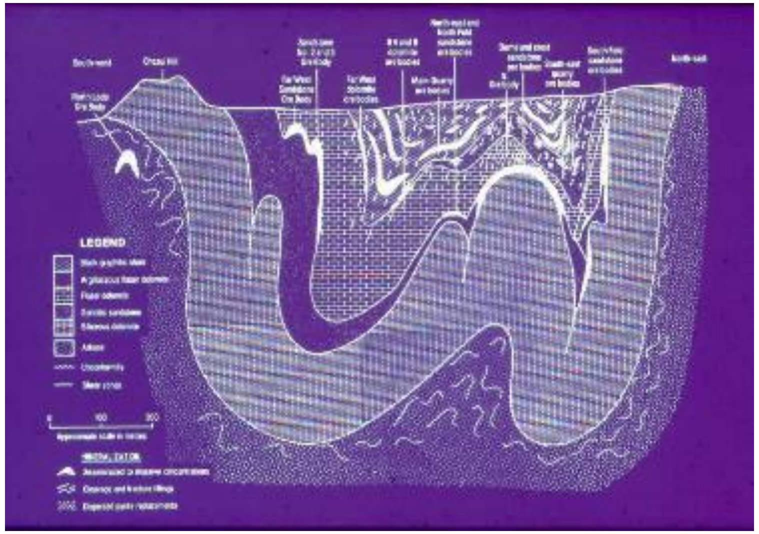


**Alaska Cu Mine, Lomagundi Group**

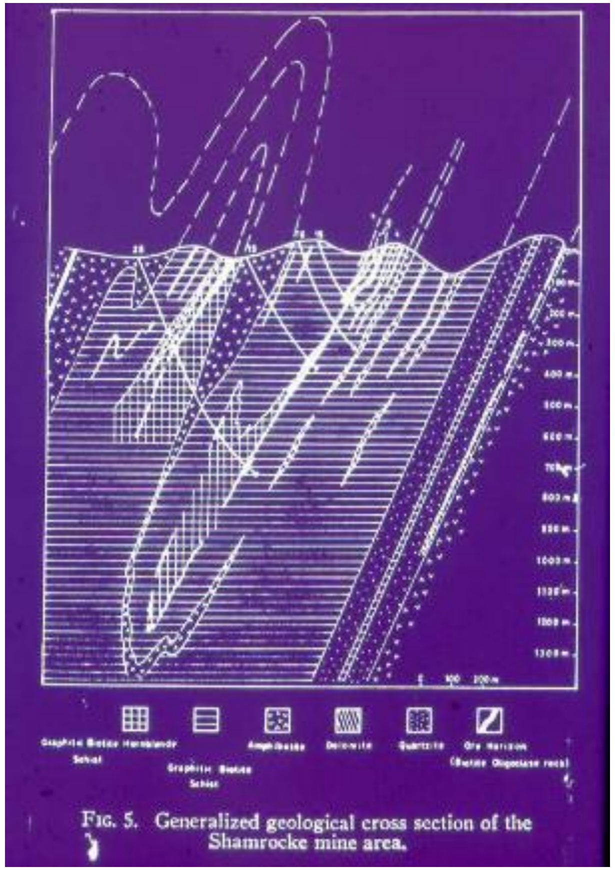


FIG. 5. Generalized geological cross section of the Shamrocke mine area.

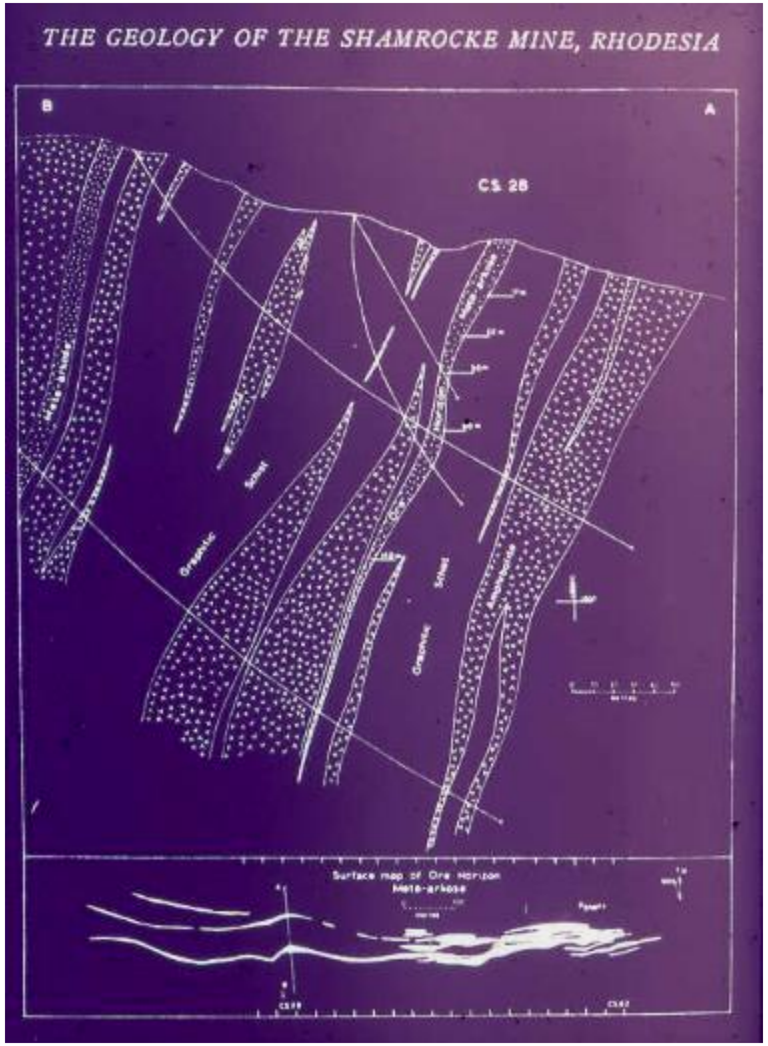


Thole, 1976, Econ. Geol.

**Shamrocke Cu Mine, Lomagundi Group**

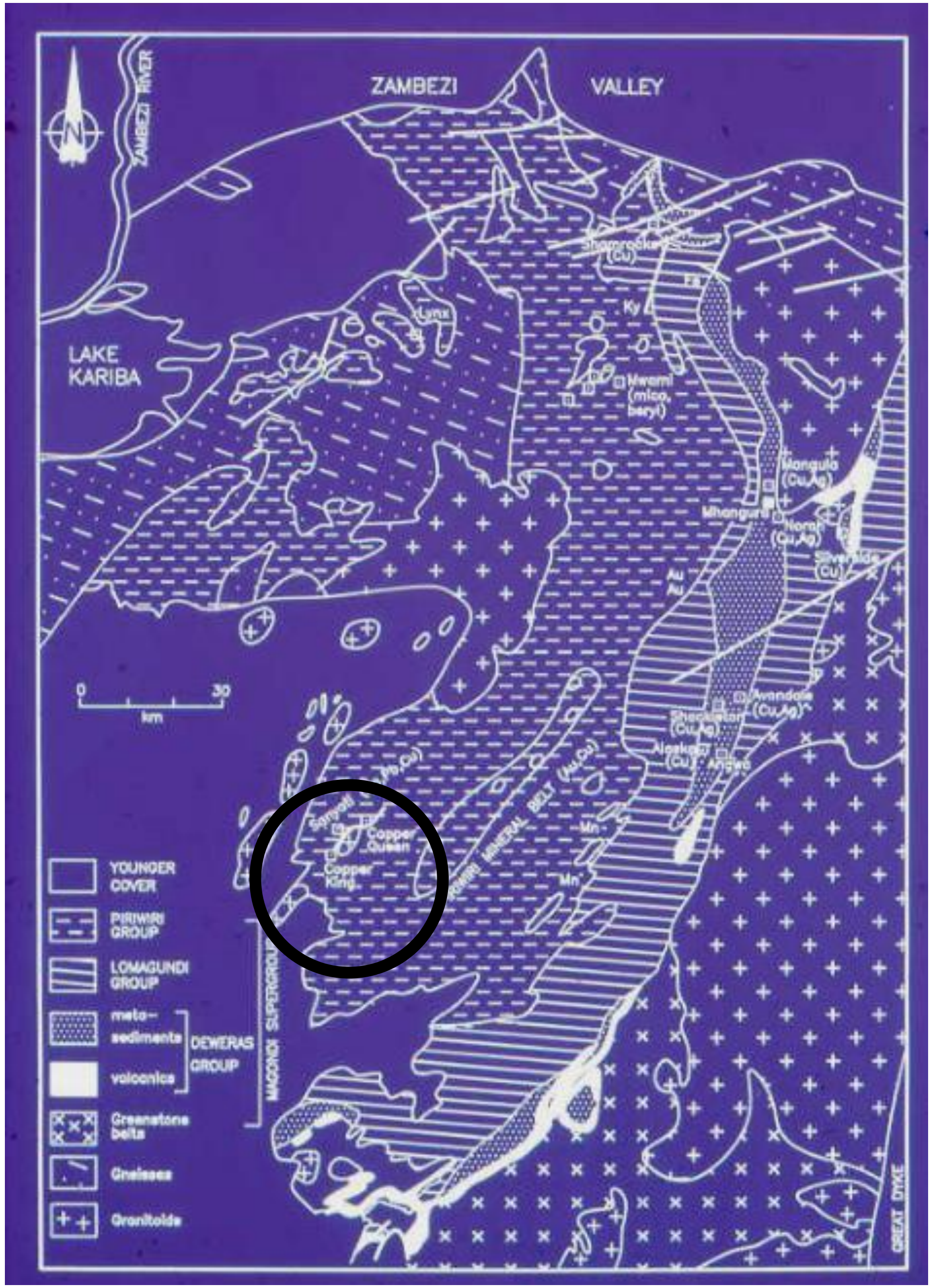


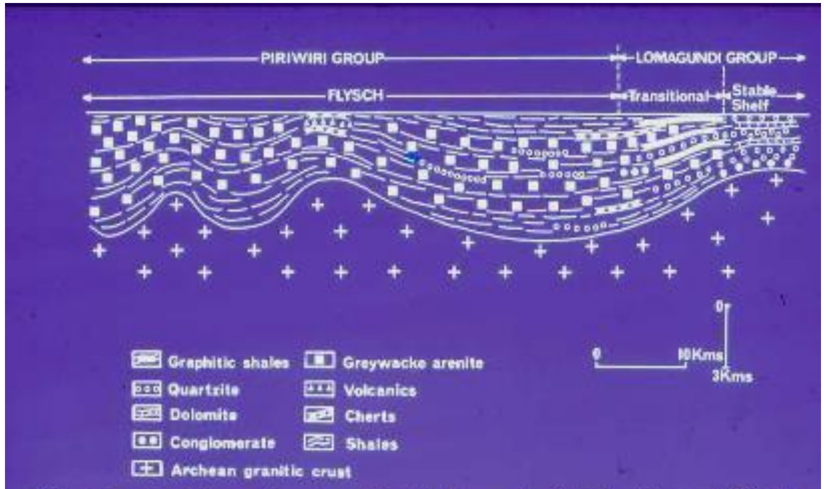

Schematic section to show sedimentary relationships between the Piriwiri and Lomagundi Groups.
Leyshon and Tennick (1988)

**Piriwiri Group**: Deeper water facies turbiditic equivalent of the Lomagundi Group carbonate shelf

Copper Queen sediment-hosted massive sulphide Cu-Zn-(Pb-Ag) deposits

# PIRIWIRI GROUP

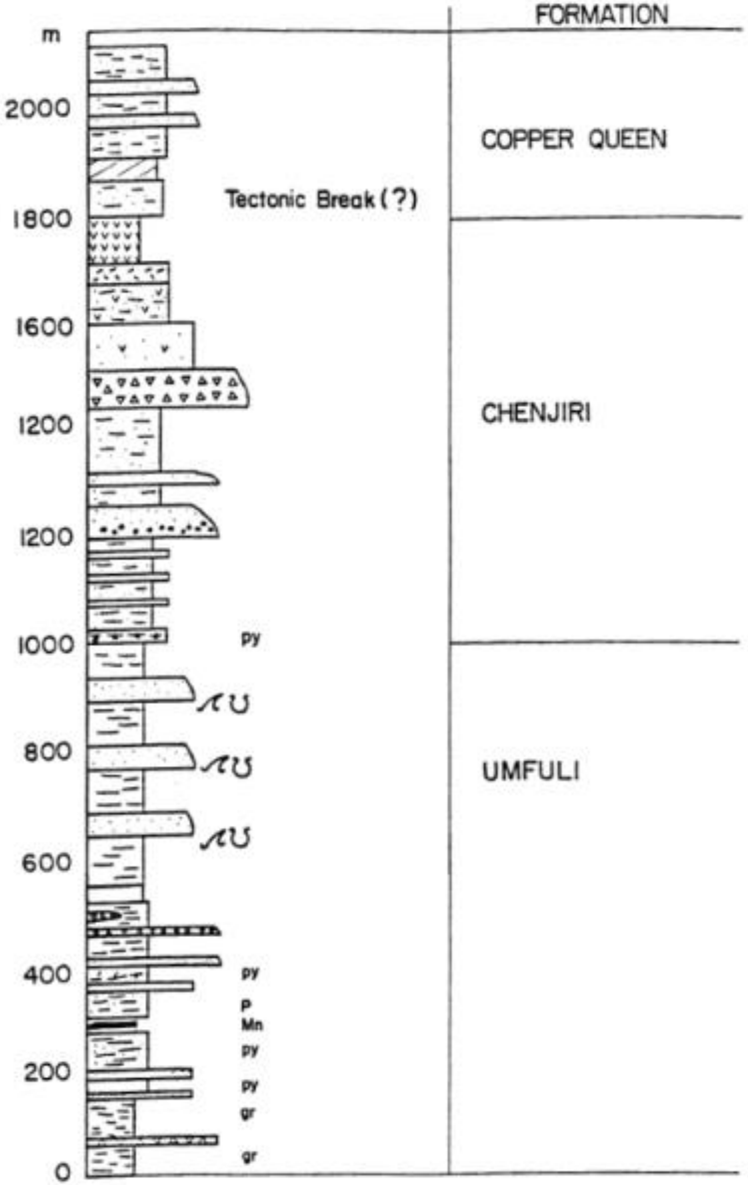


## KEY

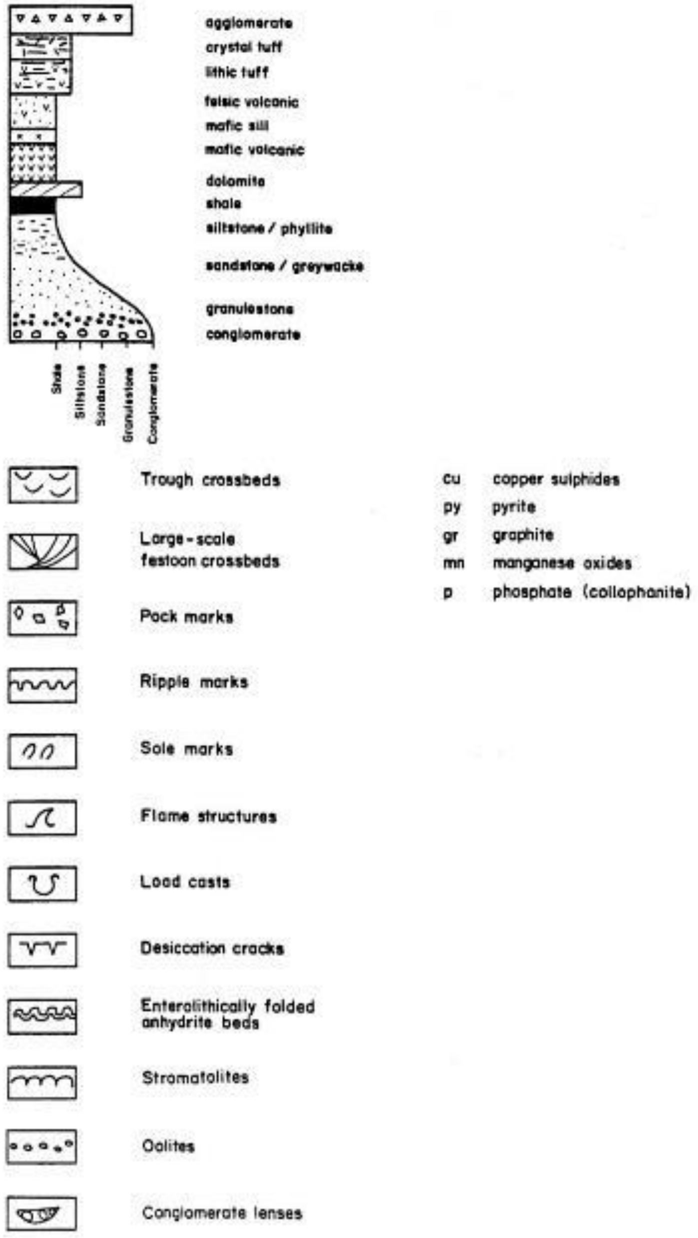

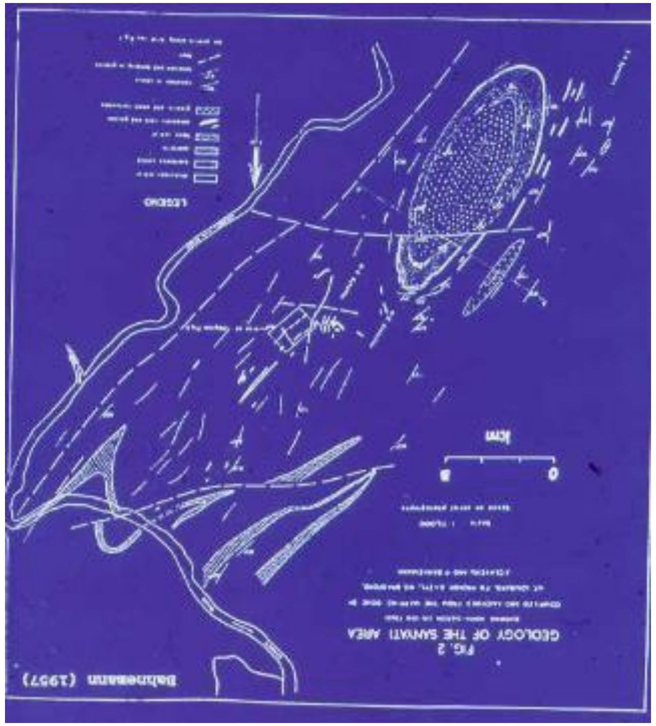


# Copper Queen Cu-Zn-(Pb)-(Ag) SHMS deposit, Piriwiri Group

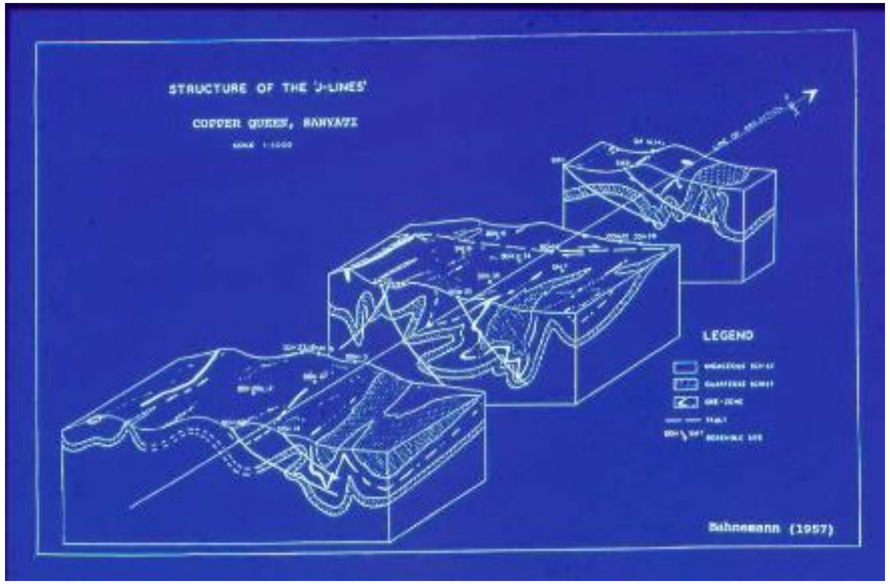


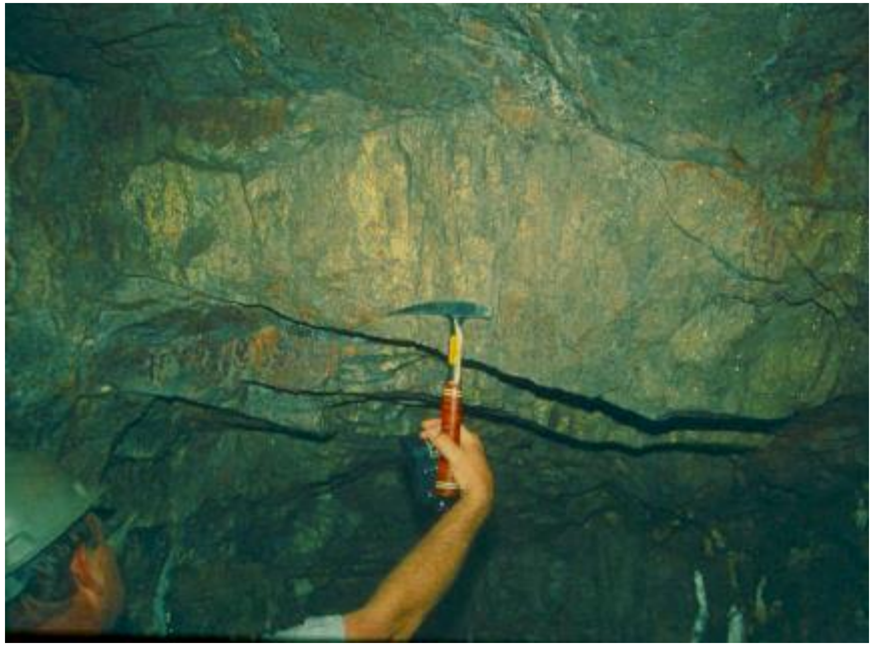

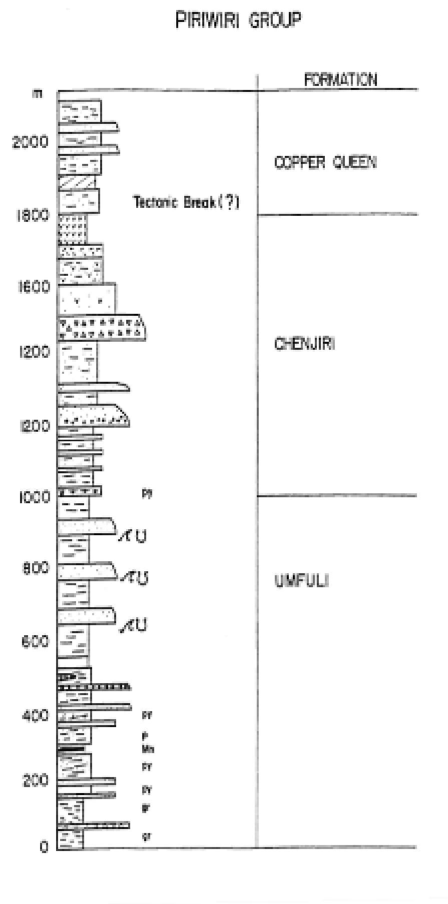


Chenjiri Fm, in upper part of Piriwiri Group- calc-alkaline agglomerates and felsites- mark the approach of a magmatic arc which collided during the Magondi Orogeny. Some Au mineralization associated with these volcanics in “Piriwiri mineral belt”.

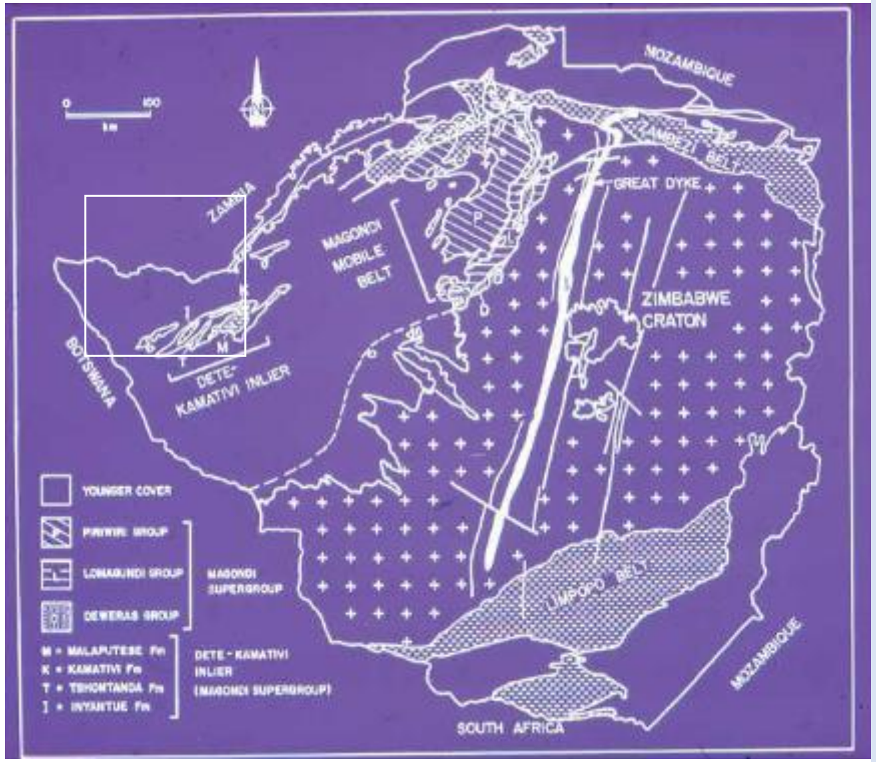


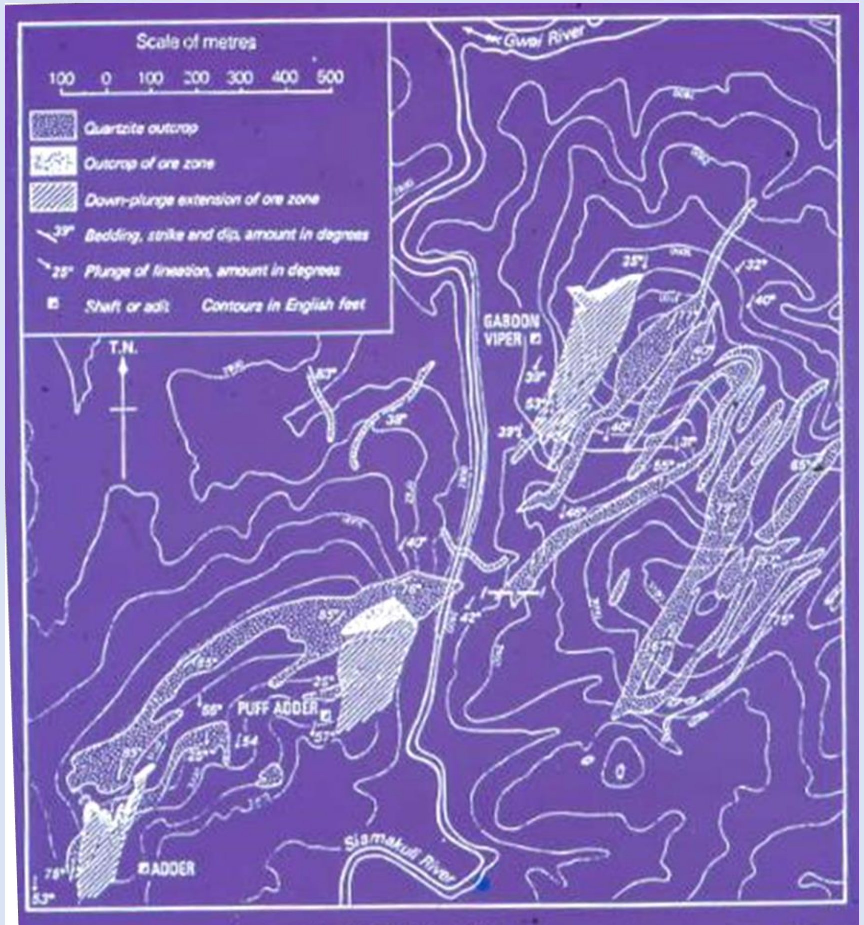


FIG. 12. Map showing ore shoots in relation to quartzite outcrops, Gwaai River Mine.

Lockett (1979)

**Gneisses, Kamativi**

**Gwaai River Cu Mine**, Dete-Kamativi Inlier: Synmetamorphic replacement of pyritic interflow metasediments by chalcopyrite in fold hinges

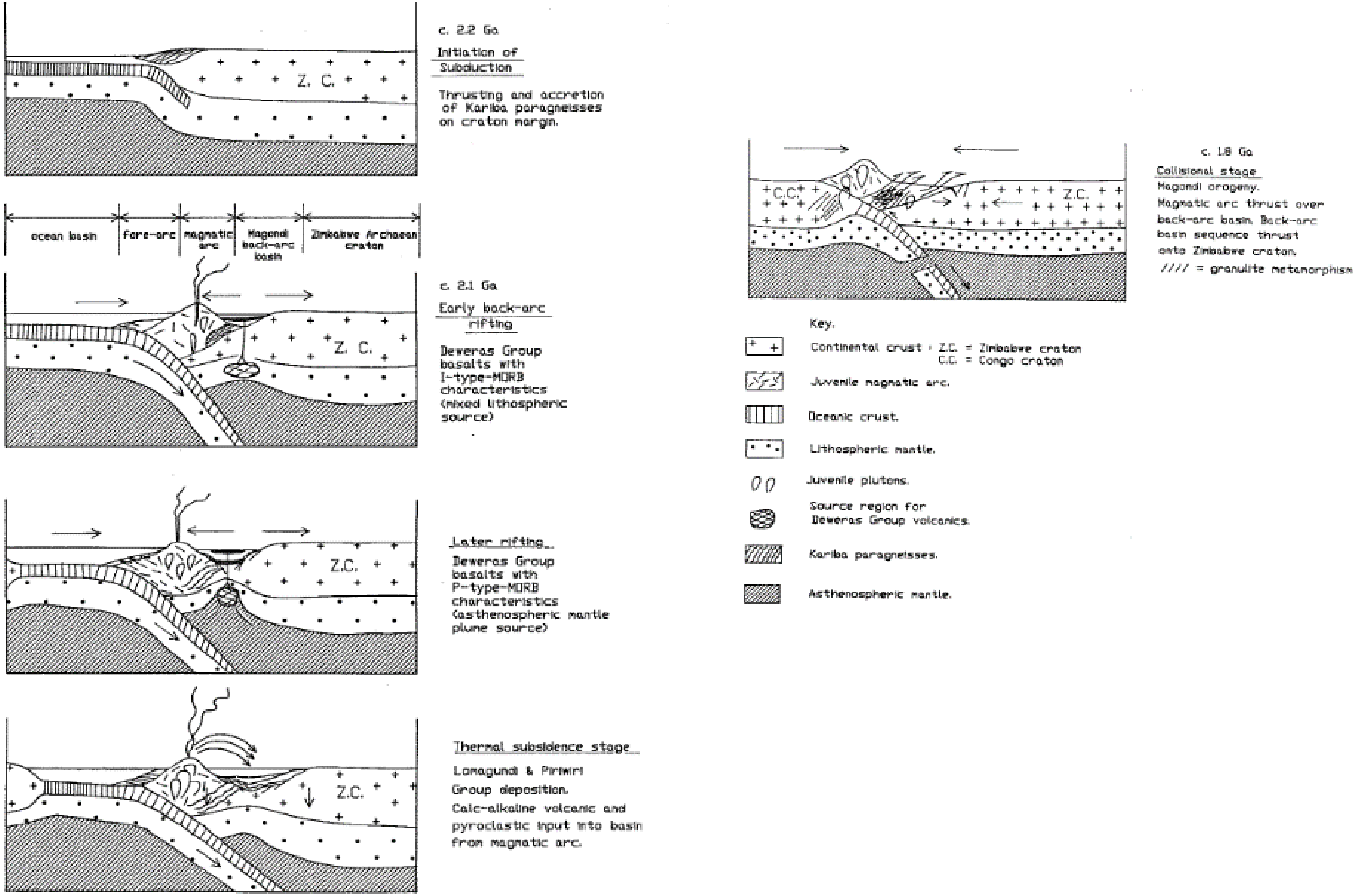
c. 2.2 Ga
Initiation of Subduction
Thrusting and accretion of Kariba paragneisses on craton margin.
Z. C.
ocean basin
fore-arc
magmatic arc
Magondi back-arc basin
Zimbabwe Archaean craton
c. 2.1 Ga
Early back-arc rifting
Deweras Group basalts with I-type-MORB characteristics (mixed lithospheric source)
Z. C.
Later rifting
Deweras Group basalts with P-type-MORB characteristics (asthenospheric mantle plume source)
Z.C.
Thermal subsidence stage
Lomagundi & Piriwiri Group deposition.
Calc-alkaline volcanic and pyroclastic input into basin from magmatic arc.
Z.C.
c. 1.8 Ga
Collisional stage
Magondi orogeny.
Magmatic arc thrust over back-arc basin. Back-arc basin sequence thrust onto Zimbabwe craton.
//// = granulite metamorphism
C.C.
Z.C.
Key.
Continental crust : Z.C. = Zimbabwe craton
C.C. = Congo craton
Juvenile magmatic arc.
Oceanic crust.
Lithospheric mantle.
Juvenile plutons.
Source region for Deweras Group volcanics.
Kariba paragneisses.
Asthenospheric mantle.

# Highbury Impact Structure, Zimbabwe

**False Colour Composite (bands 4,3,2 in RGB order)**

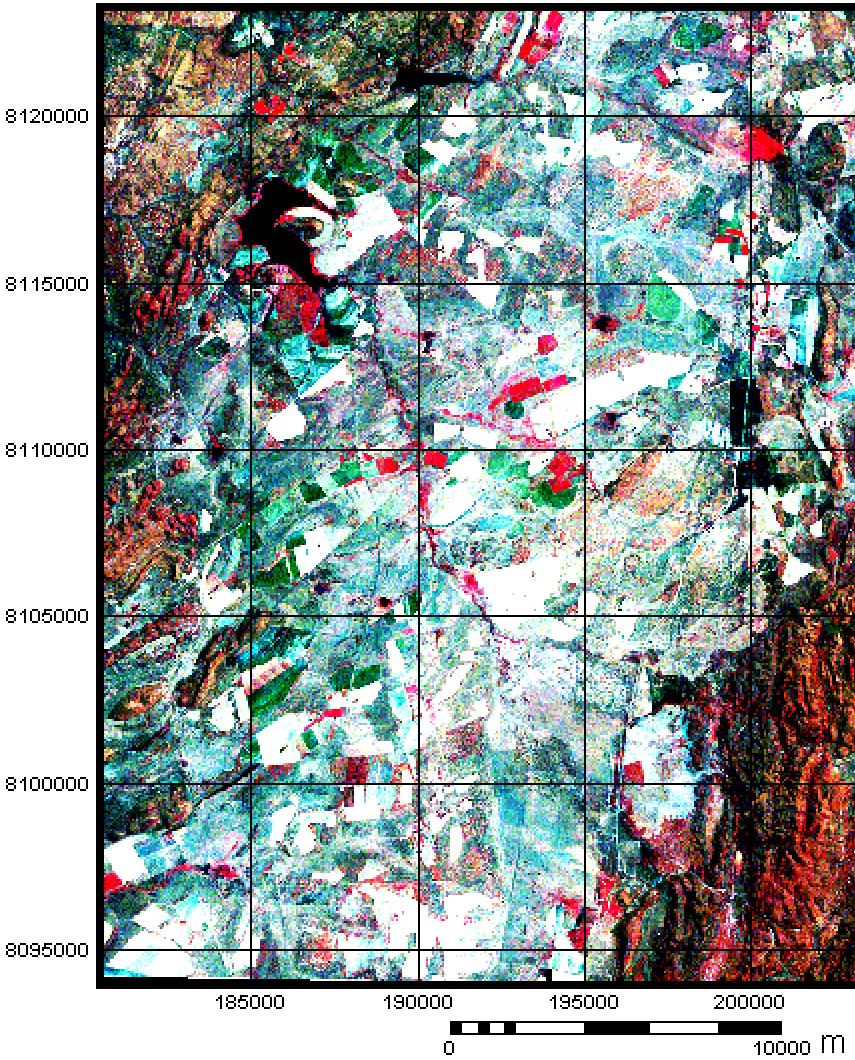


Master et al. 1994, 1995.

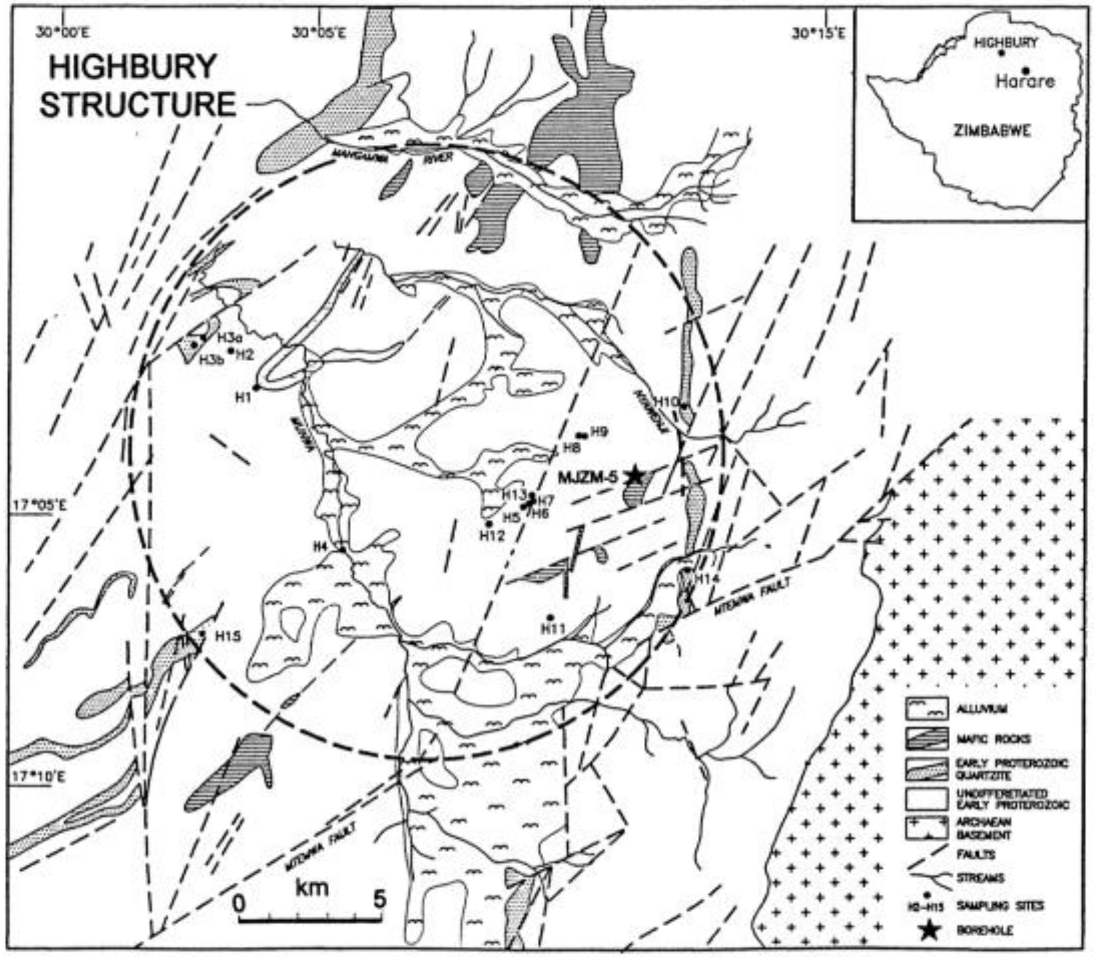


Figure 1: Simplified geological map of the Highbury Structure (dashed circle), after Stagman (1961) [6].

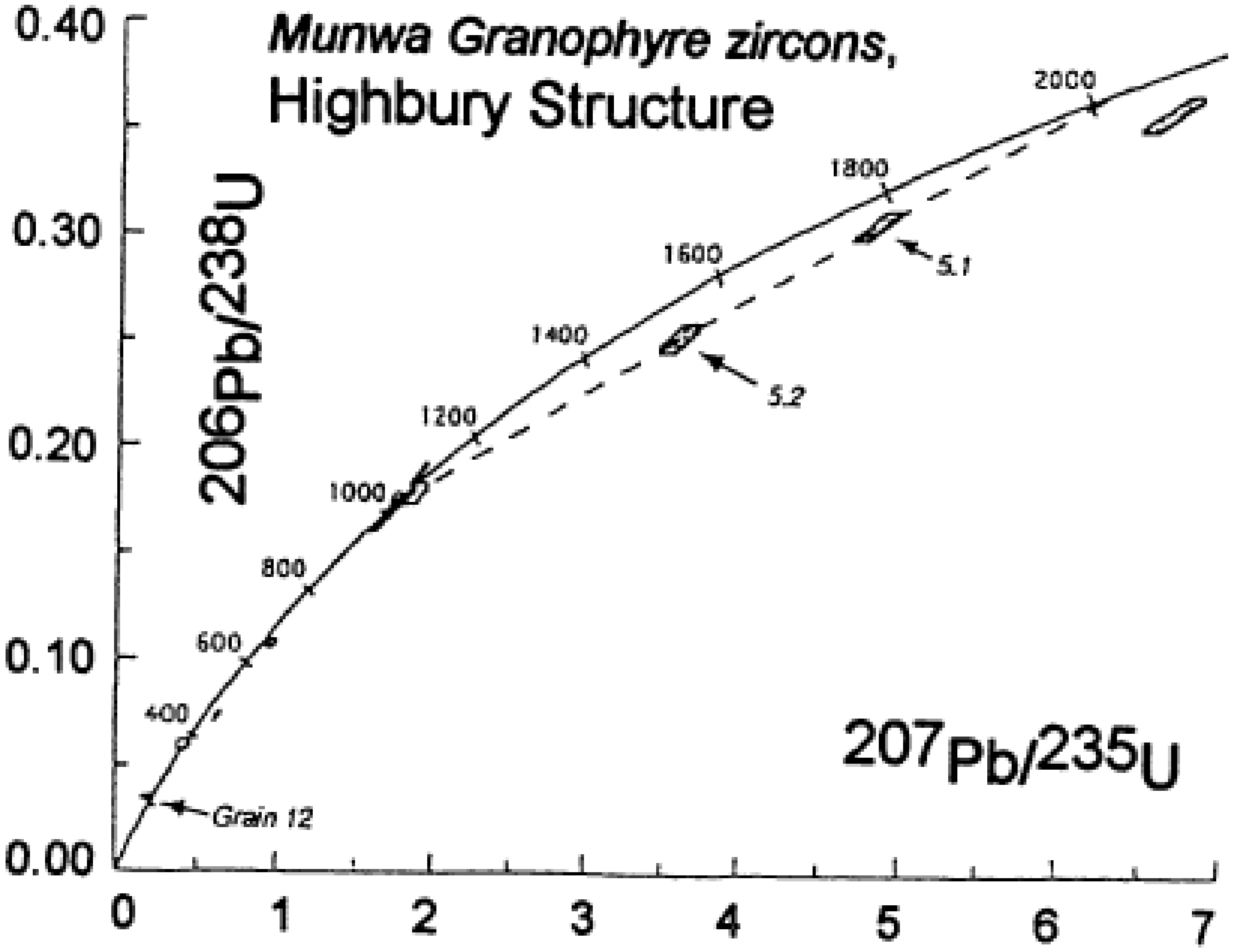


# Age of Highbury Impact: 1034 ± 13 Ma

SHRIMP U-Pb age on zircons

Master et al., 1995, LPSC 16.

# West Magondi Belt Magmatic Arc

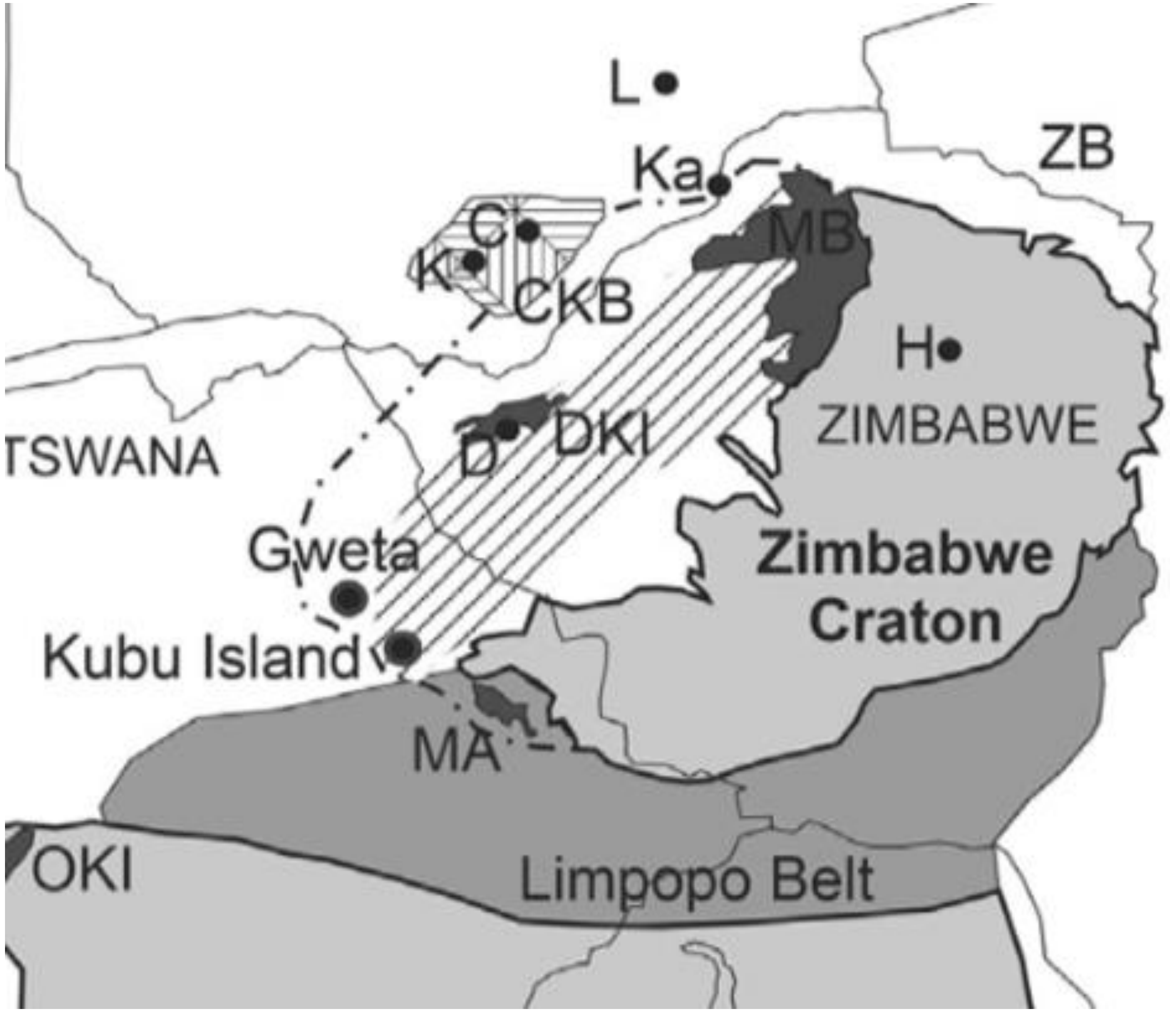

# Our new geochronological data from the Magondi "basement"

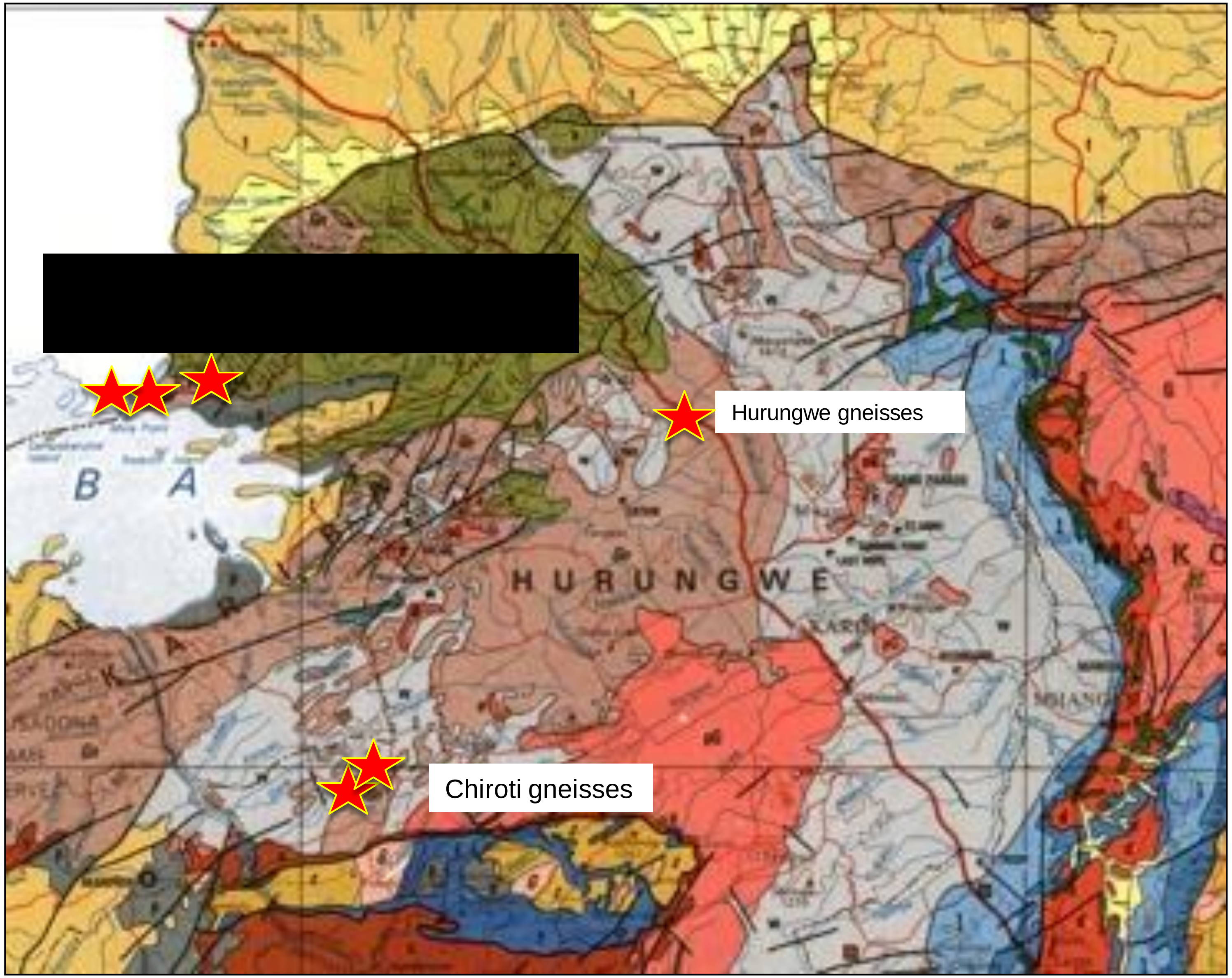

ZMB13/6

Chiroti Gneiss II


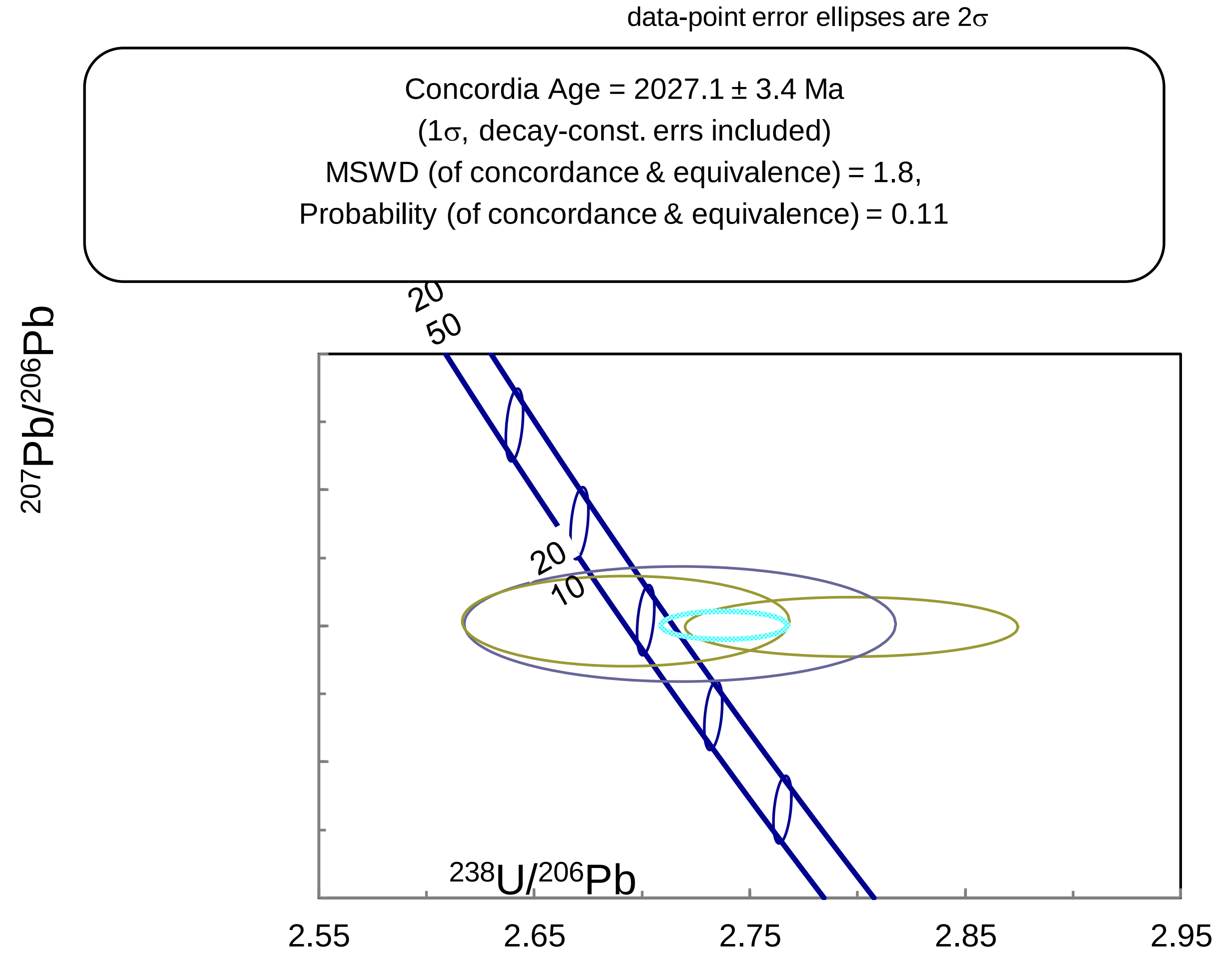


Age of intrusion of Chiroti Gneiss II is **2027.1± 2.7 Ma**

ZMB13/5  Chiroti Augen Gneiss

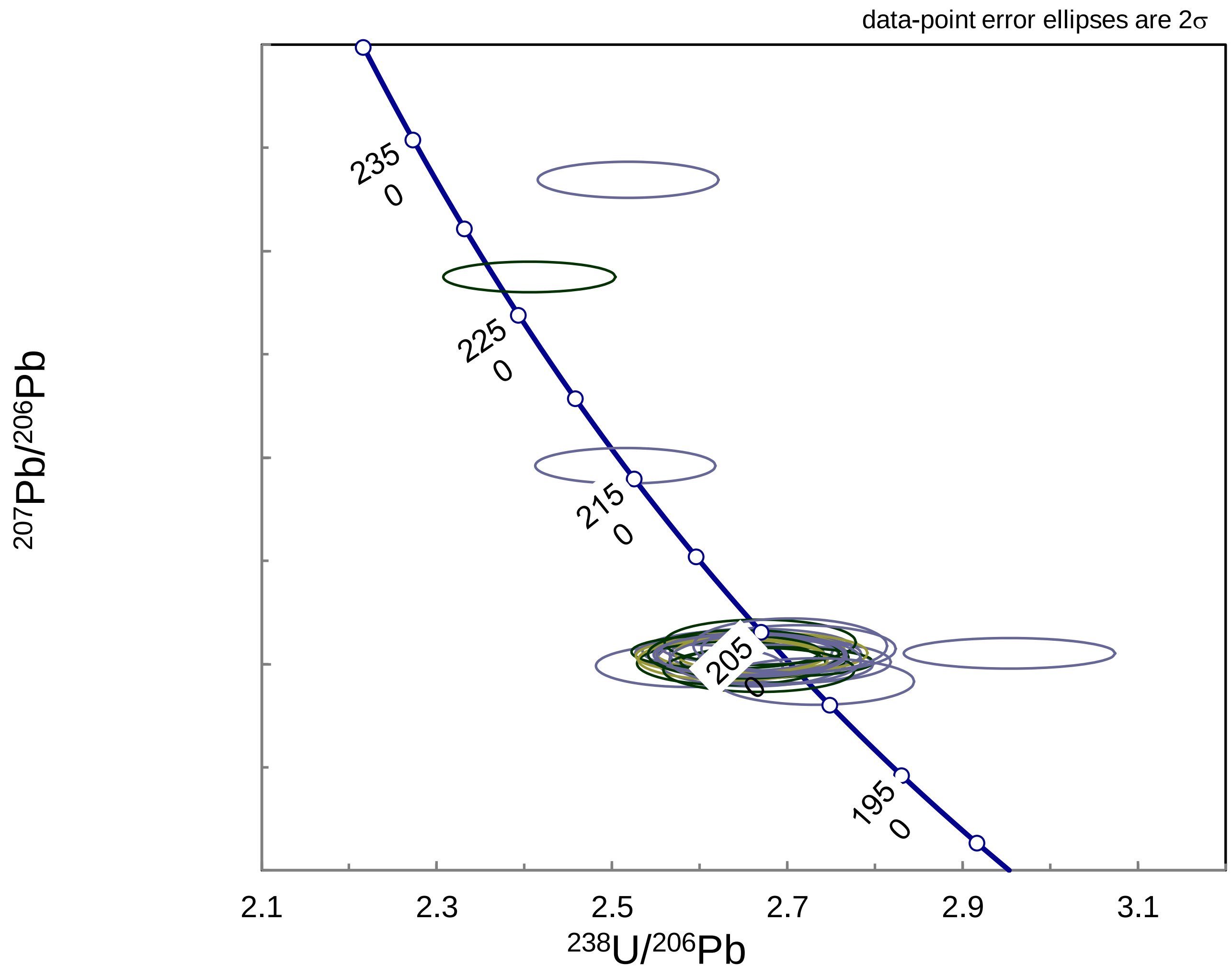


Chiroti Augen Gneiss ZMB13/5 Age: 2038.9 ± 2.7 Ma

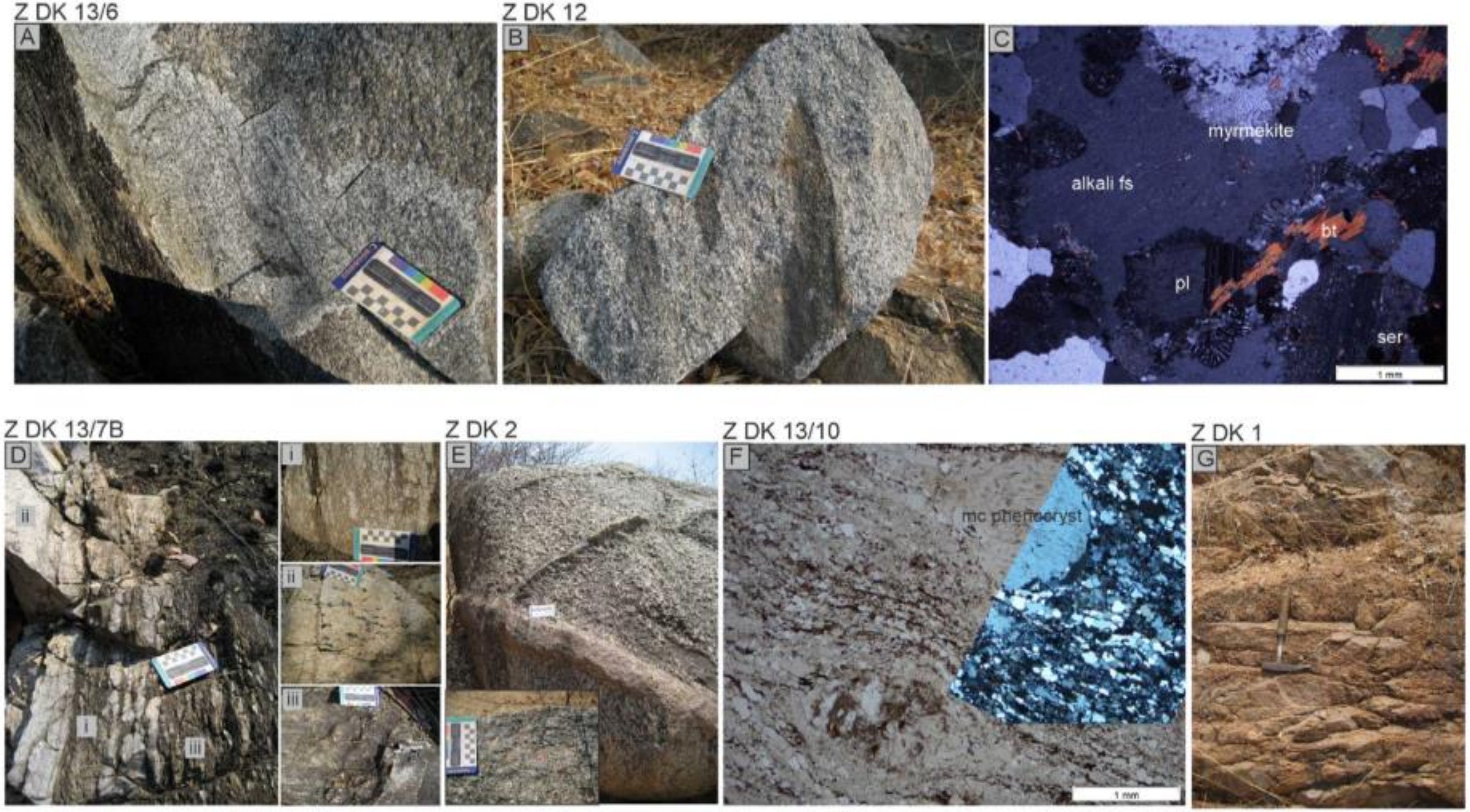


**Fig. 8.** (A) Outcrop of orthogneiss Z DK 13/6, showing the thin, dark, biotite-rich bands which define the foliation, which is also folded. (B) Outcrop of biotite orthogneiss Z DK 12, showing mafic xenoliths flattened and elongated parallel to foliation. (C) Photomicrograph of Z DK 12 depicting alteration as a result of late stage fluids which have produced myrmekitic textures along many of the feldspar grain boundaries. Retrograde metamorphism has also taken place, as recorded by the biotite which has been largely replaced by Fe-rich chlorite. (D) Outcrop of Z DK 13/7B, a heterogeneous biotite gneiss, in which three different phases can be recognised (i). Fine-grained biotite-bearing quartzofeldspathic gneiss; (ii). Quartzofeldspathic pegmatite; and (iii). Biotite gneiss. (E) Outcrop of weakly-foliated, porphyritic granitoid gneiss, Z DK 2, with a 12-cm wide slanting aplite dyke, just below the scale. Inset: close up of the porphyritic granitoid gneiss, showing pink K-feldspar phenocrysts. (F) Composite photomicrograph of augen orthogneiss Z DK 13/10, showing a plane-polarised view (main photograph), and cross-polarised view (right) of the thin section, indicating foliated fine-grained quartz-feldspar aggregates curved around microcline phenocrysts which have been transformed into augen via shearing. (G) Outcrop of pink leucogranite Z DK 1, which consists of abundant quartz in addition to large grains of muscovite and microcline feldspar, lending it a pinkish tinge.

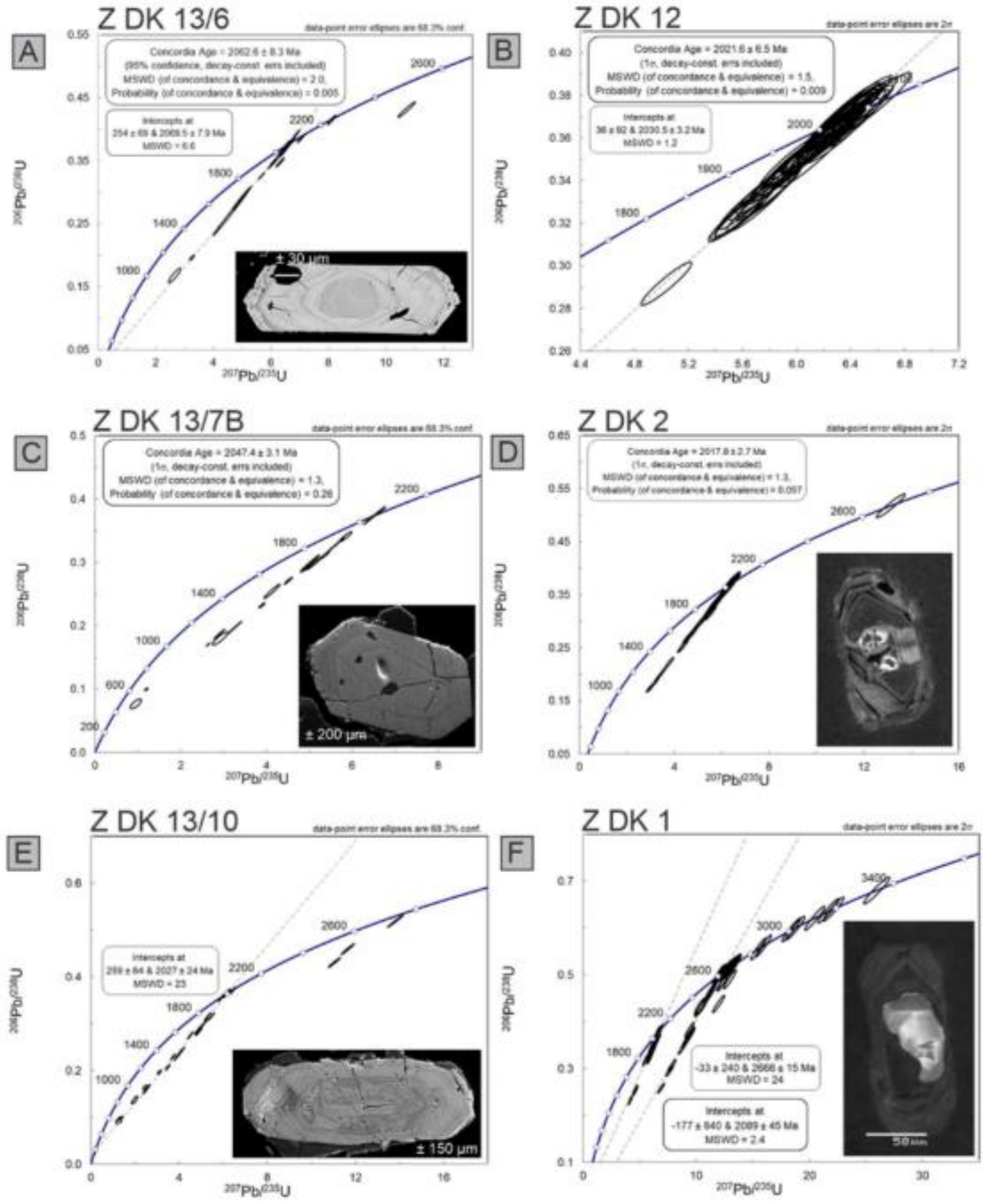

Z DK 13/6
A
Concordia Age = 2062.6 ± 8.3 Ma
Intercepts at
254 ± 69 & 2069.5 ± 7.9 Ma
MSWD = 6.6
± 30 µm
Z DK 12
B
Concordia Age = 2021.6 ± 6.5 Ma
Intercepts at
36 ± 92 & 2030.5 ± 3.2 Ma
MSWD = 1.2
Z DK 13/7B
C
Concordia Age = 2047.4 ± 3.1 Ma
± 200 µm
Z DK 2
D
Concordia Age = 2017.8 ± 2.7 Ma
Z DK 13/10
E
Intercepts at
259 ± 64 & 2027 ± 24 Ma
MSWD = 23
± 150 µm
Z DK 1
F
Intercepts at
-33 ± 240 & 2666 ± 15 Ma
MSWD = 24
Intercepts at
-177 ± 840 & 2089 ± 45 Ma
MSWD = 2.4

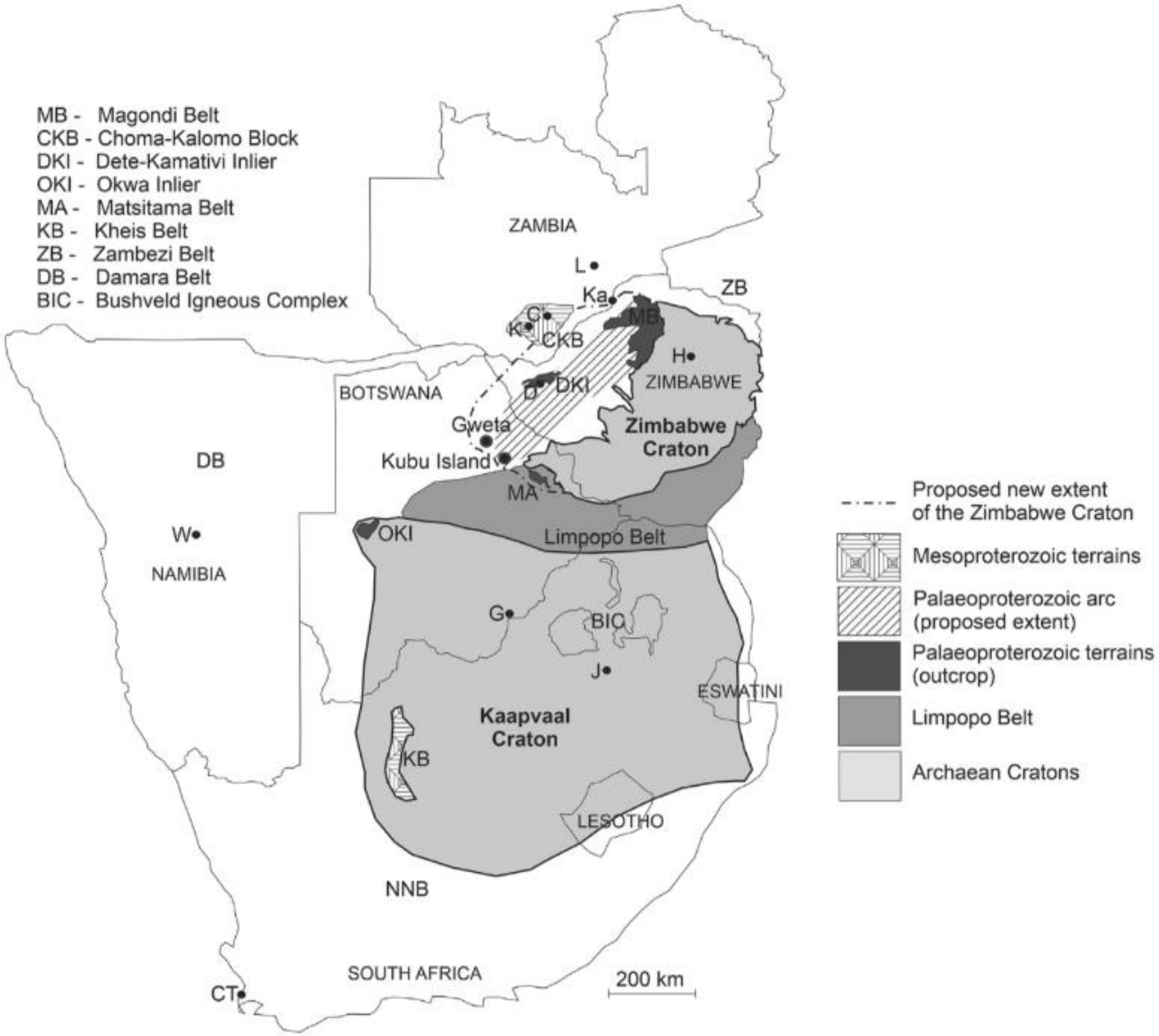


**Fig. 10.** Sketch map depicting the proposed new extent of the Archaean Zimbabwe Craton and Palaeoproterozoic magmatic arc, in relation to the Kaapvaal Craton (after Majaule et al., 2001; McCourt et al., 2001; Mapeo et al., 2004; Kramers et al., 2006; Jacobs et al., 2008; Eglington et al., 2009; Naydenov et al., 2014; Lehmann et al., 2015). Key to place names: CT – Cape Town, J – Johannesburg, G – Gaborone, W – Windhoek, D – Dete, K – Kalomo, C – Choma, H – Harare, Ka – Kariba, L – Lusaka.

Figure 7.4: Geological section, looking North, of 2284 XC/E, 4-70 Level, Norah Mine, showing fractures and veins in Norah Metadolerite Sill, and sampling sites for Rb-Sr dating (with sample numbers indicated).

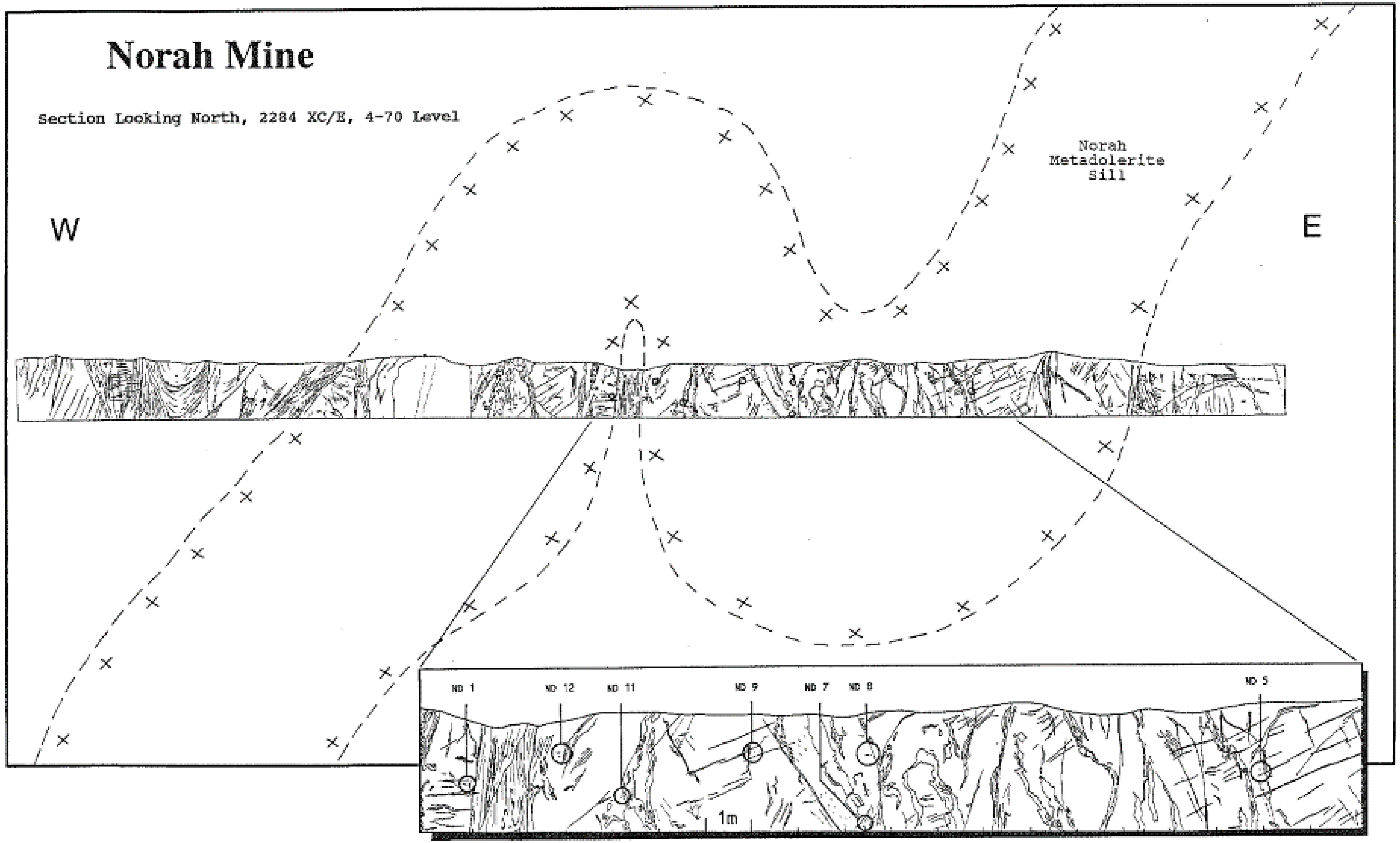

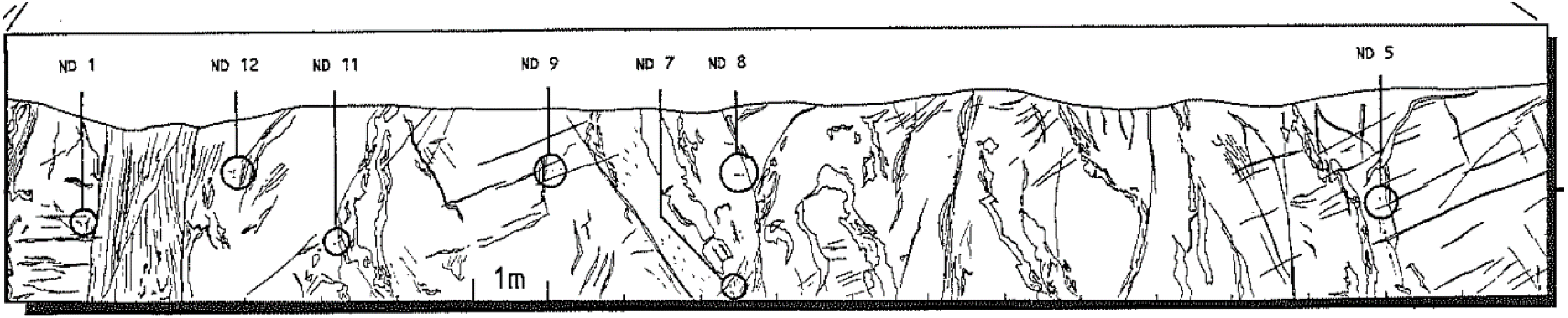


1:40 scale mapping of underground crosscut showing veins cutting the Norah Metadolerite Sill,
And locations of samples taken for Rb-Sr geochronology

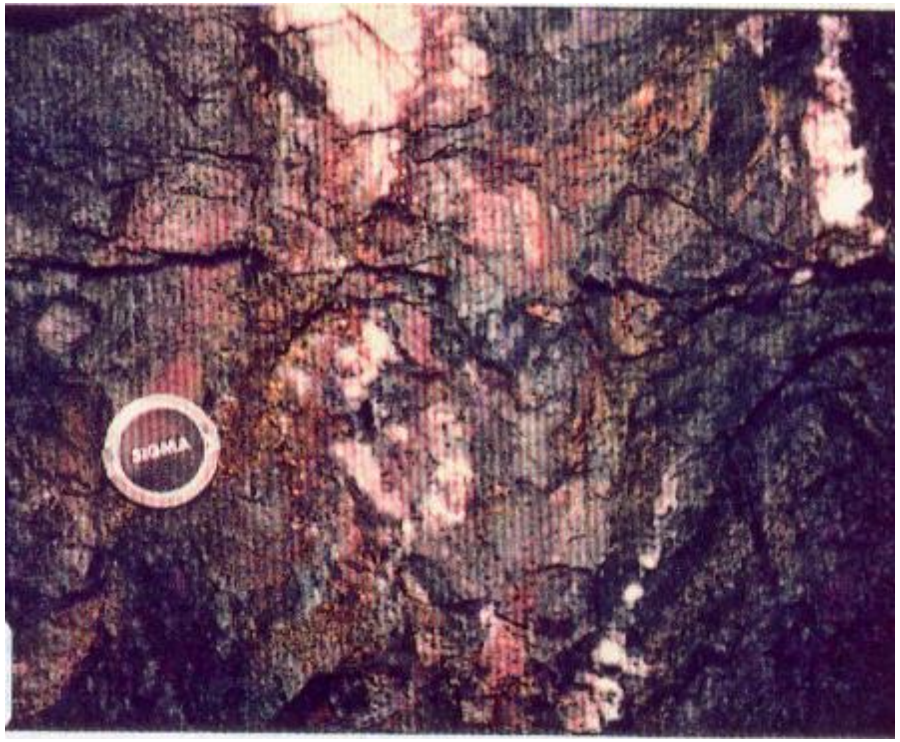


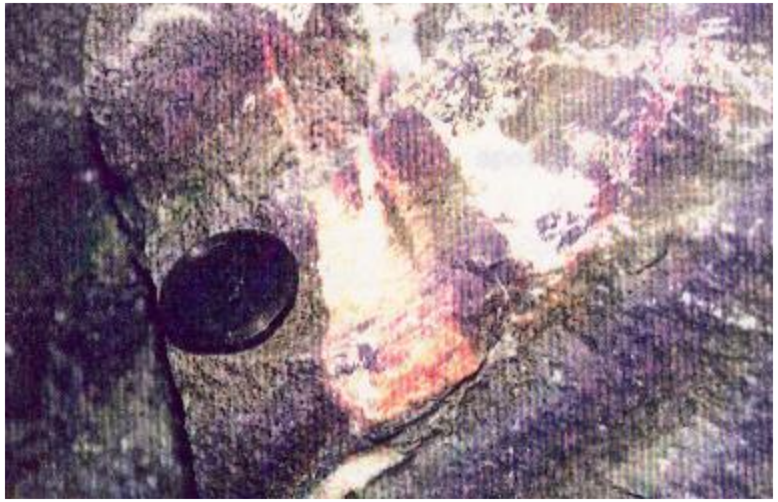

Microcline-haematite veins
in Norah metadolerite sill

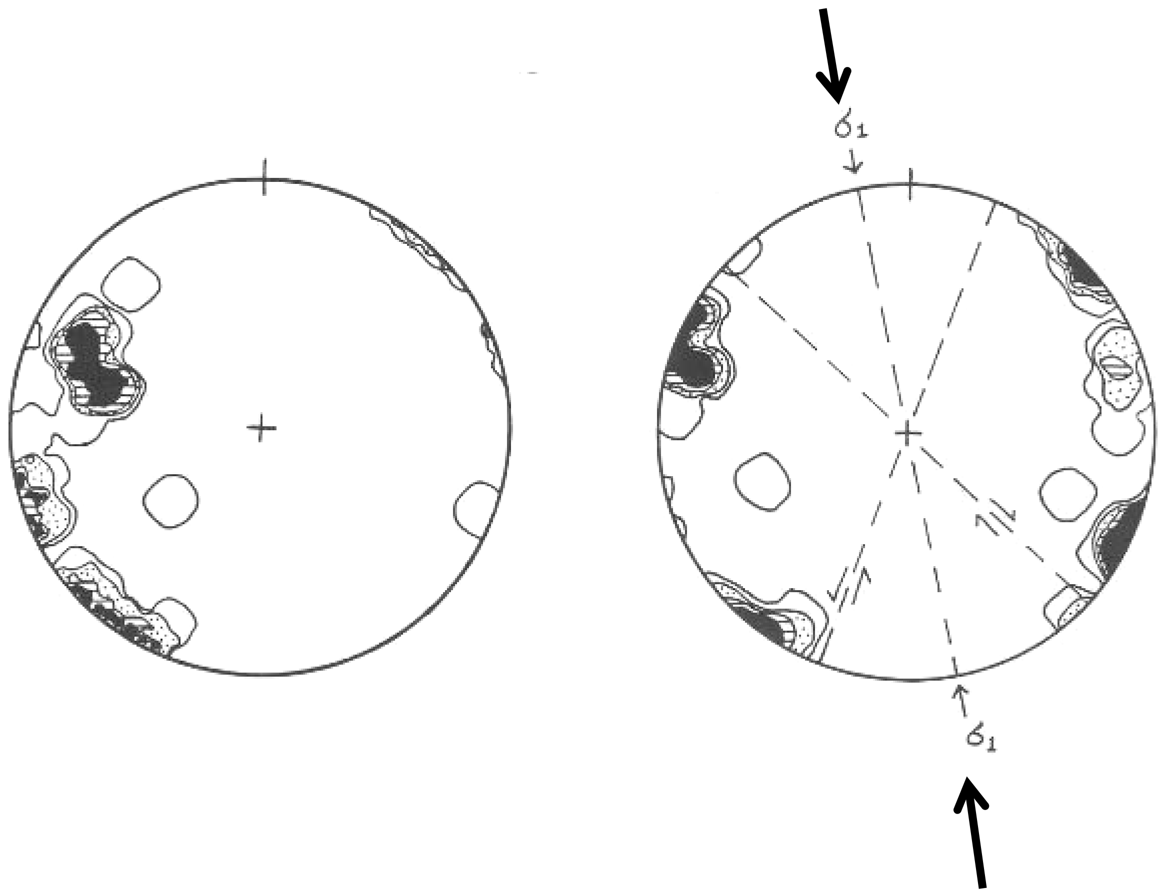


Microcline-haematite veins in Norah metadolerite sill-
NNE-SSW principal stress (σ1)- D4 deformation phase
during Pan-African Zambezi Orogeny, c. 550 Ma

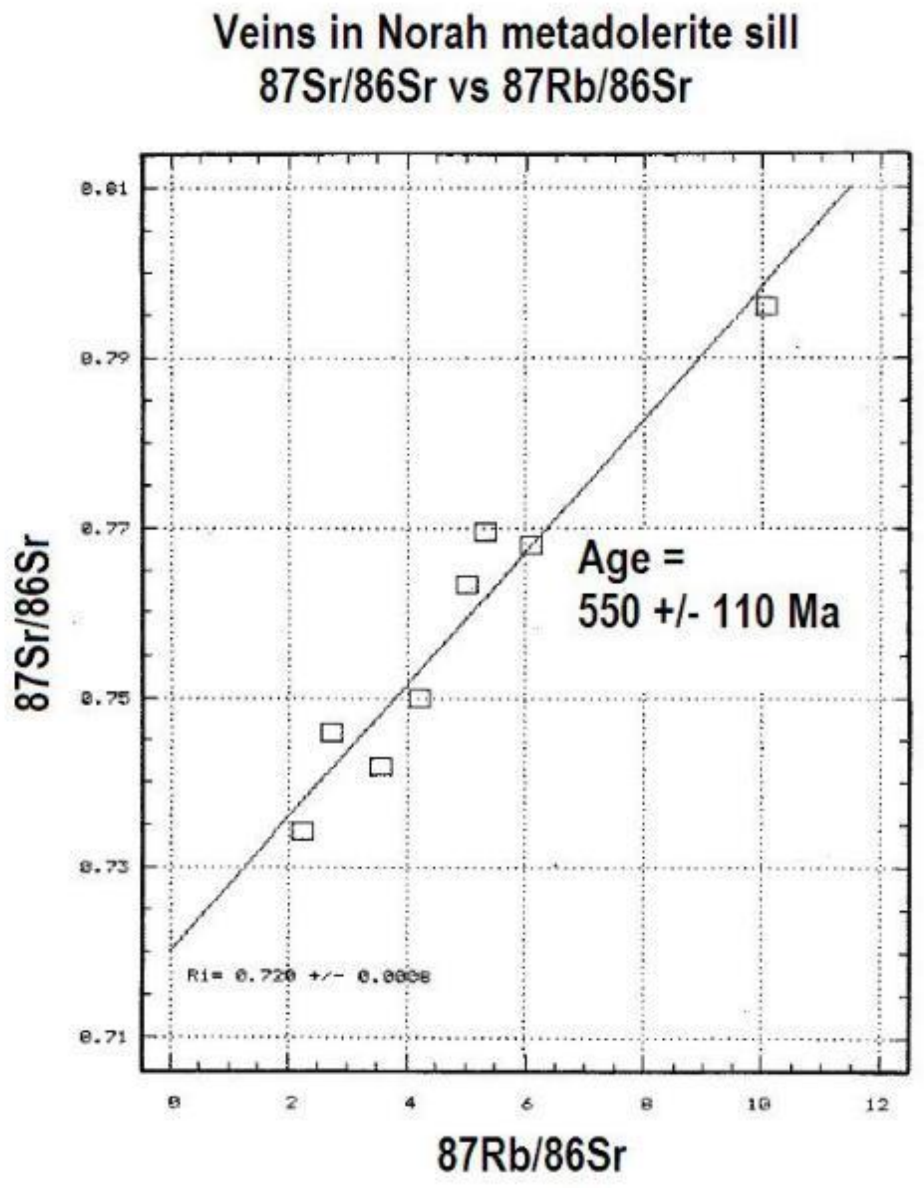


Master, S. & Kramers, J.D. (2000). A structural and Rb-Sr study of metamorphic veins from the Palaeoproterozoic Magondi Belt, Zimbabwe: implications for the nature and origin of Pan-African overprinting. *J. Afr. Earth Sci*., **30(4A)**, p. 60.


**Finally, Congo and Kalahari Cratons collide in Damara-Lufilian-Zambezi Orogeny at 590-522 Ma, during the Pan-African assembly of the Gondwana Supercontinent**

(after K. Burke, 2005)

# Carbon isotopes

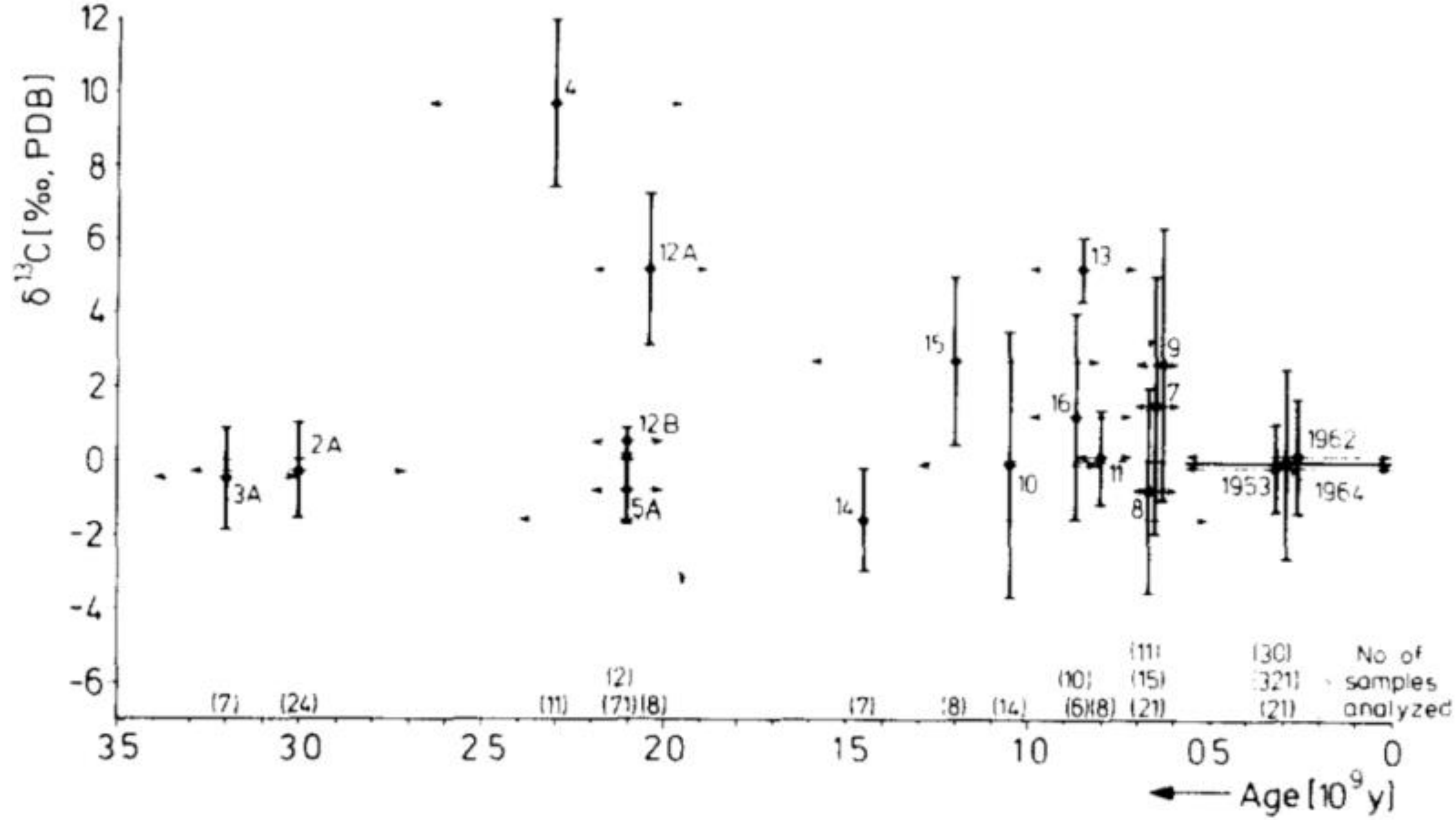


Schidlowski et al., 1975

Fig.11. Carbon isotope composition of substantially unaltered sedimentary carbonates as a function of geologic time. Mean $\delta^{13}C$ values of carbonate groups investigated are indicated by circles, the vertical bars representing the standard deviation; horizontal arrows show possible geological time range. Numbers refer to Tables IIA—XVI listing the values yielded by individual samples of each group or locality. (Values for Phanerozoic carbonates (< 0.57 $10^9$y) according to Craig, 1953; Degens and Epstein, 1962; Keith and Weber, 1964.)

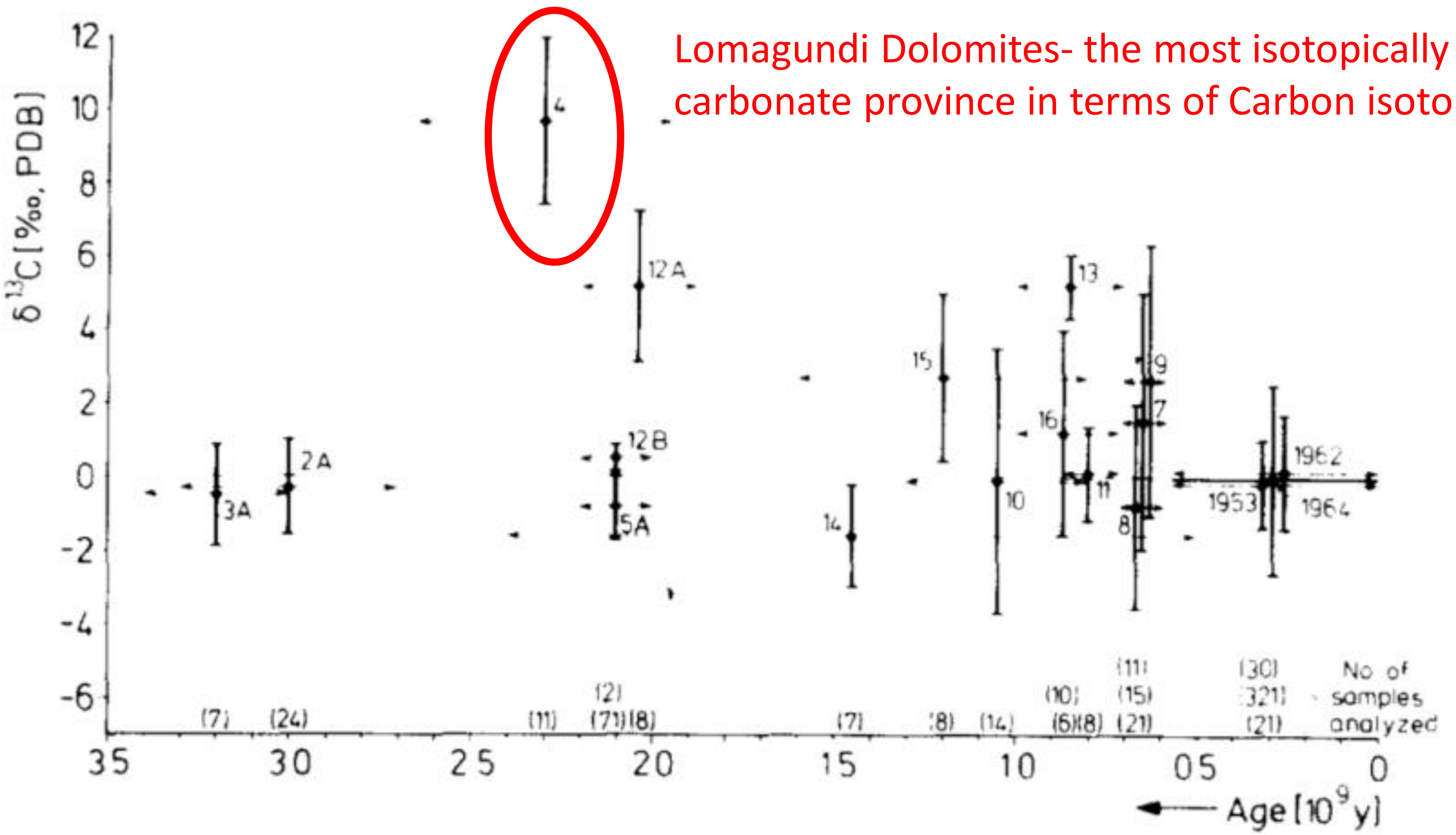


Lomagundi Dolomites- the most isotopically anomalous carbonate province in terms of Carbon isotopes

Schidlowski et al., 1975

Fig. 11. Carbon isotope composition of substantially unaltered sedimentary carbonates as a function of geologic time. Mean $\delta^{13}C$ values of carbonate groups investigated are indicated by circles, the vertical bars representing the standard deviation; horizontal arrows show possible geological time range. Numbers refer to Tables IIA—XVI listing the values yielded by individual samples of each group or locality. (Values for Phanerozoic carbonates (< 0.57 $10^9$y) according to Craig, 1953; Degens and Epstein, 1962; Keith and Weber, 1964.)

# Carbon isotopes of sedimentary carbonate rocks from the Lomagundi Group

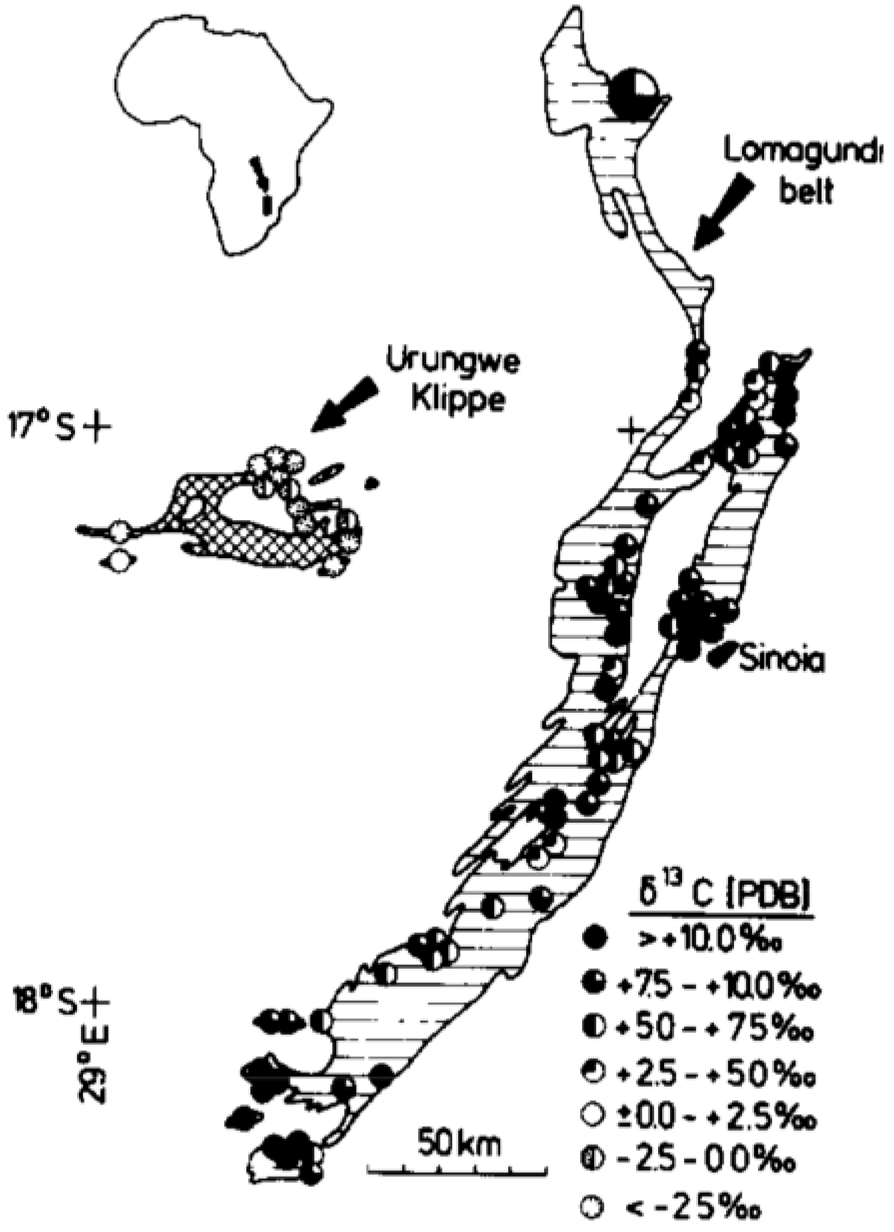


Schidlowski et al., 1976

In a reconnaissance isotopic study of global Precambrian carbonates, by Schidlowski et al. (1975), the carbonate rocks of the Lomagundi Group were found to be the most isotopically anomalous regional carbonate province in the world, being very enriched in $^{13}C$, with an average $\delta^{13}C$ value of +8.2‰ VPDB.

Subsequent work in the Magondi Basin has shown that high $\delta^{13}C$ carbonates are also present in the continental rocks of the underlying Deweras Group.

**The "Lomagundi Event" has now been recognized globally in carbonate rocks deposited in the time span 2.2-2.06 Ga.**

# “Lomagundi” carbon isotope excursion- Global perturbation of the Carbon Cycle

**Figure 1. Variation in isotopic composition of carbon in sedimentary carbonates and organic matter during Paleoproterozoic time. Sources of isotopic and age data are given in Table 1. Mean $\delta^{13}C$ values of carbonates from Fennoscandian Shield from Karhu (1993) are indicated by open circles; data for all other carbonate units listed in Table 1 are indicated by closed circles. Vertical bars represent ±1 standard deviation of $\delta^{13}C$ values, and horizontal bars indicate uncertainty in age of each stratigraphic unit. Arrows combine dated formations that are either preceded or followed by major $\delta^{13}C$ shift. BIF denotes field for iron and manganese formations. Note that uncertainties given for ages do not necessarily cover uncertainties in entire depositional periods of sample groups. PDB—Peedee belemnite.**

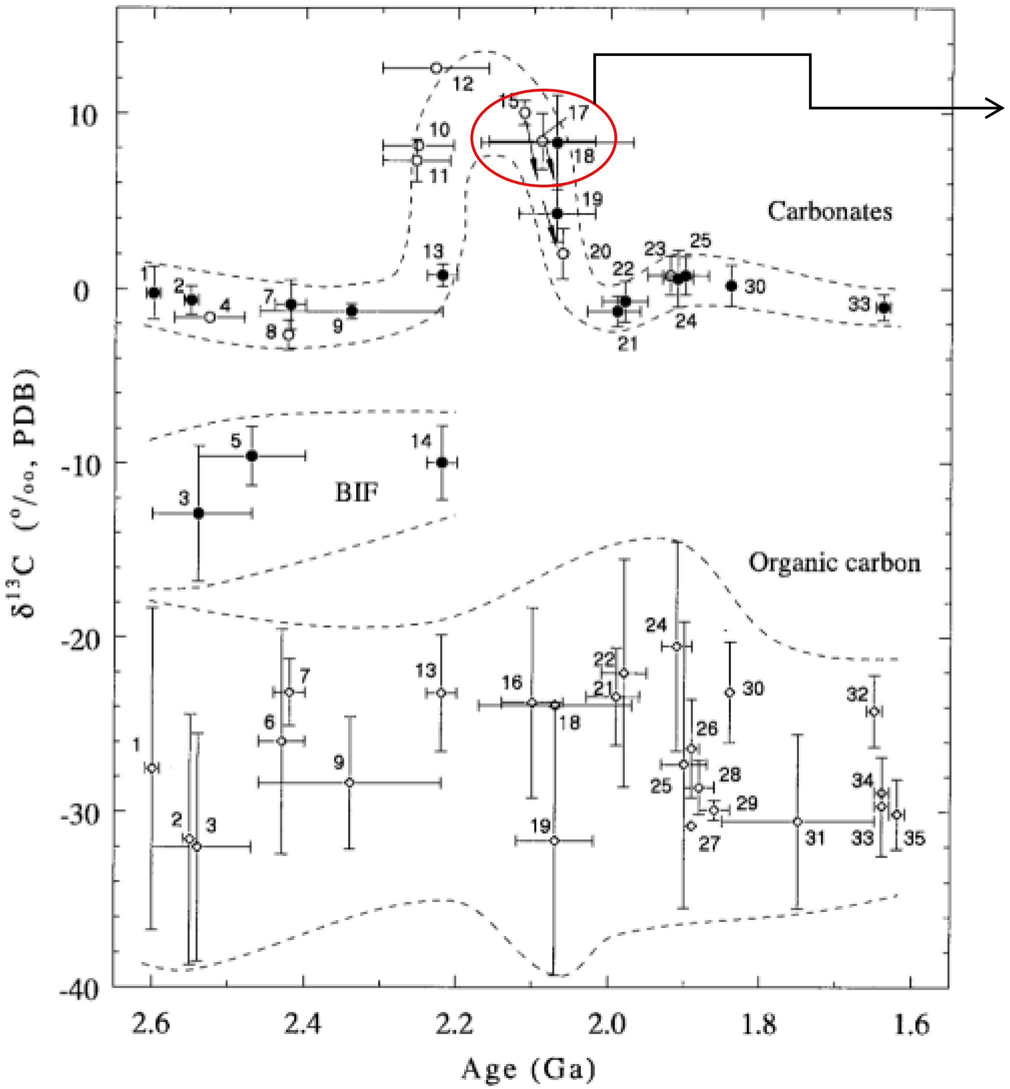


Lomagundi Group

Karhu & Holland, 1996
*Geology*

Carbonates form prominent horizons in the lower Lomagundi Group, occur in the Deweras Group as thick packages in the northern part of the basin, but form only thin lenses elsewhere, and are quite rare in the Piriwiri Group.

Sulphate pseudomorphs and beds of anhydrite are relatively common in the Deweras Group, and also occur in the Lomagundi group.

- The Magondi basin developed from continental rift to passive margin (and later to a foreland basin), and in the marine successions there are represented both proximal shallow water and distal deep water facies, and in all facies there are $^{13}C$-enriched carbonate rocks.

Master, Verhagen, Bekker
Unpublished data

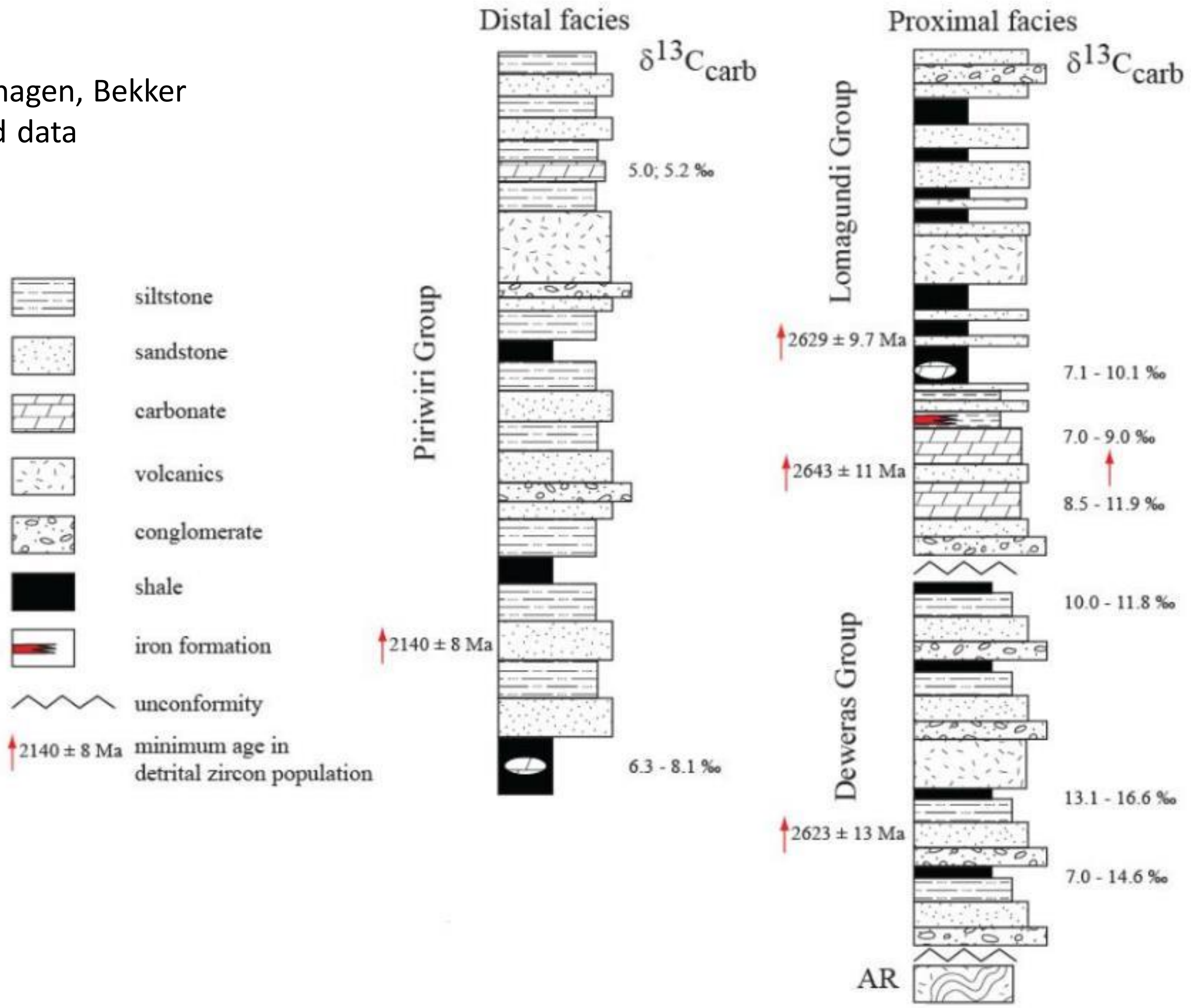

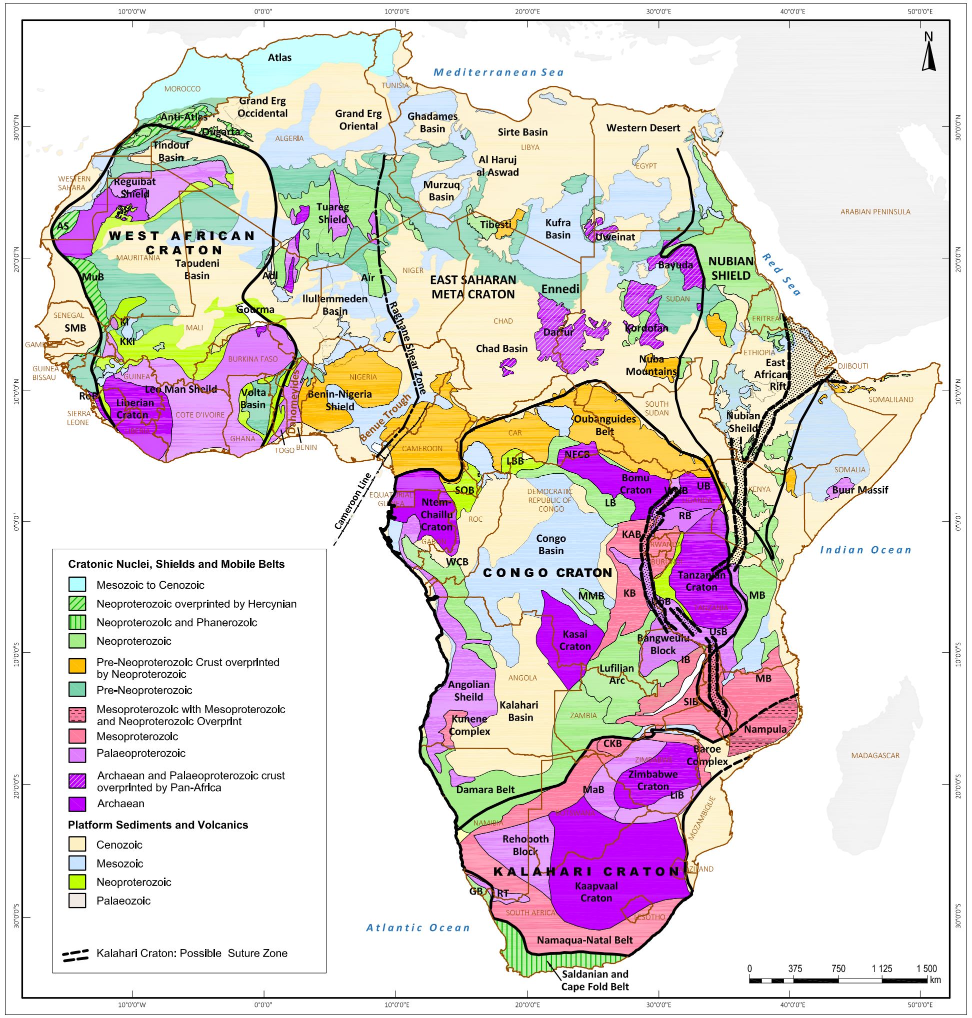


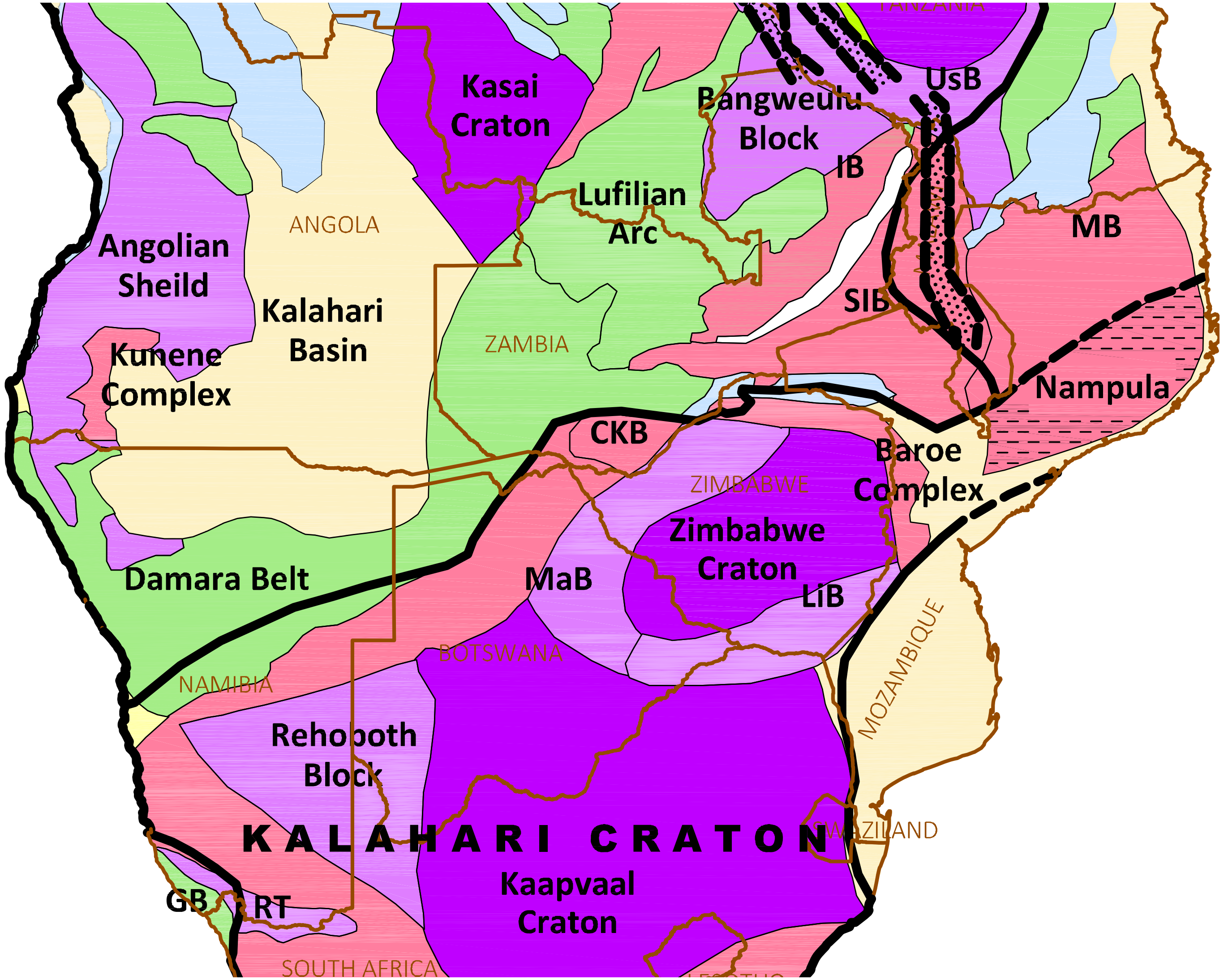


Frost-Kiliian, Master, Viljoen, Wilson (2016). Episodes

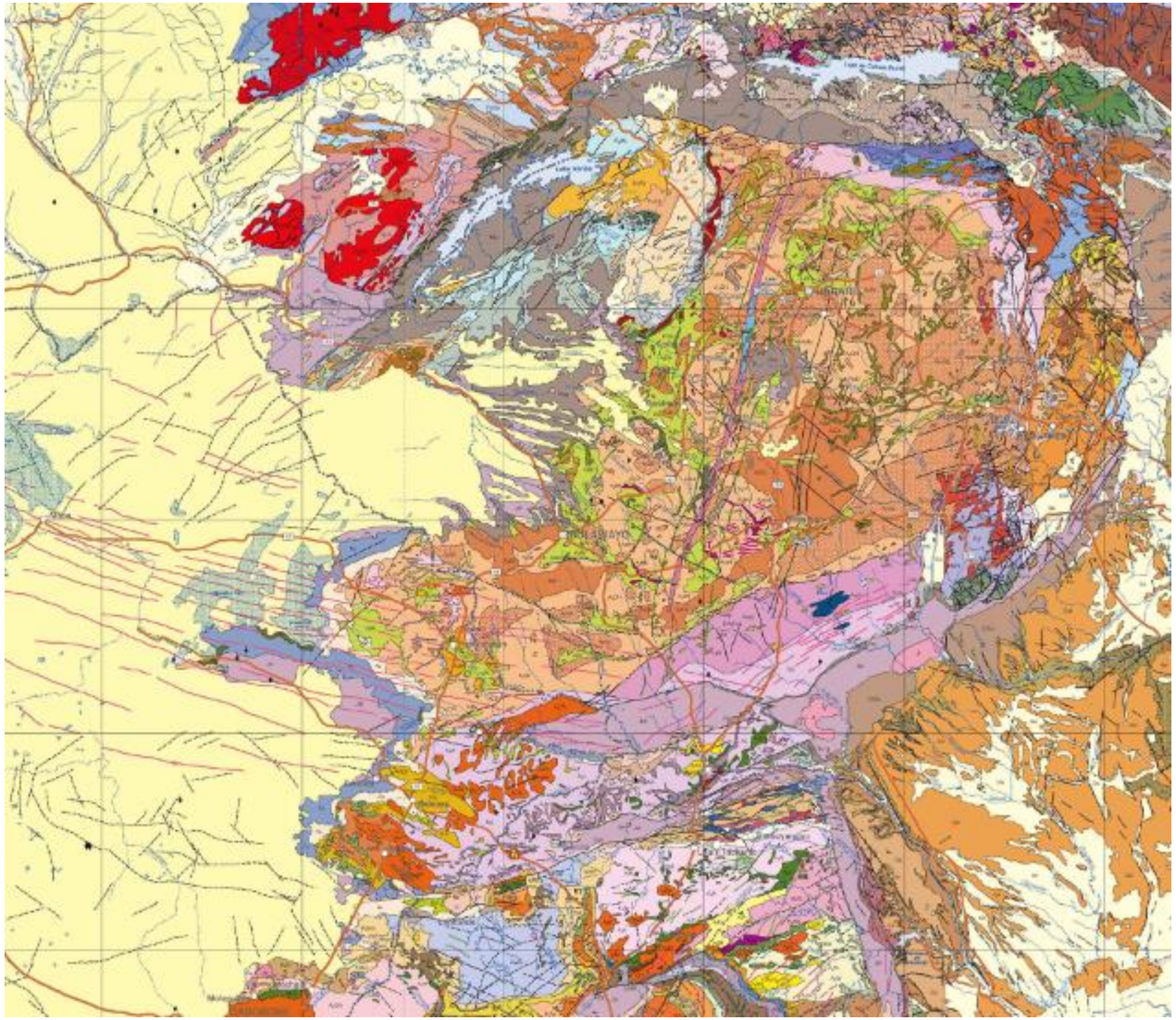

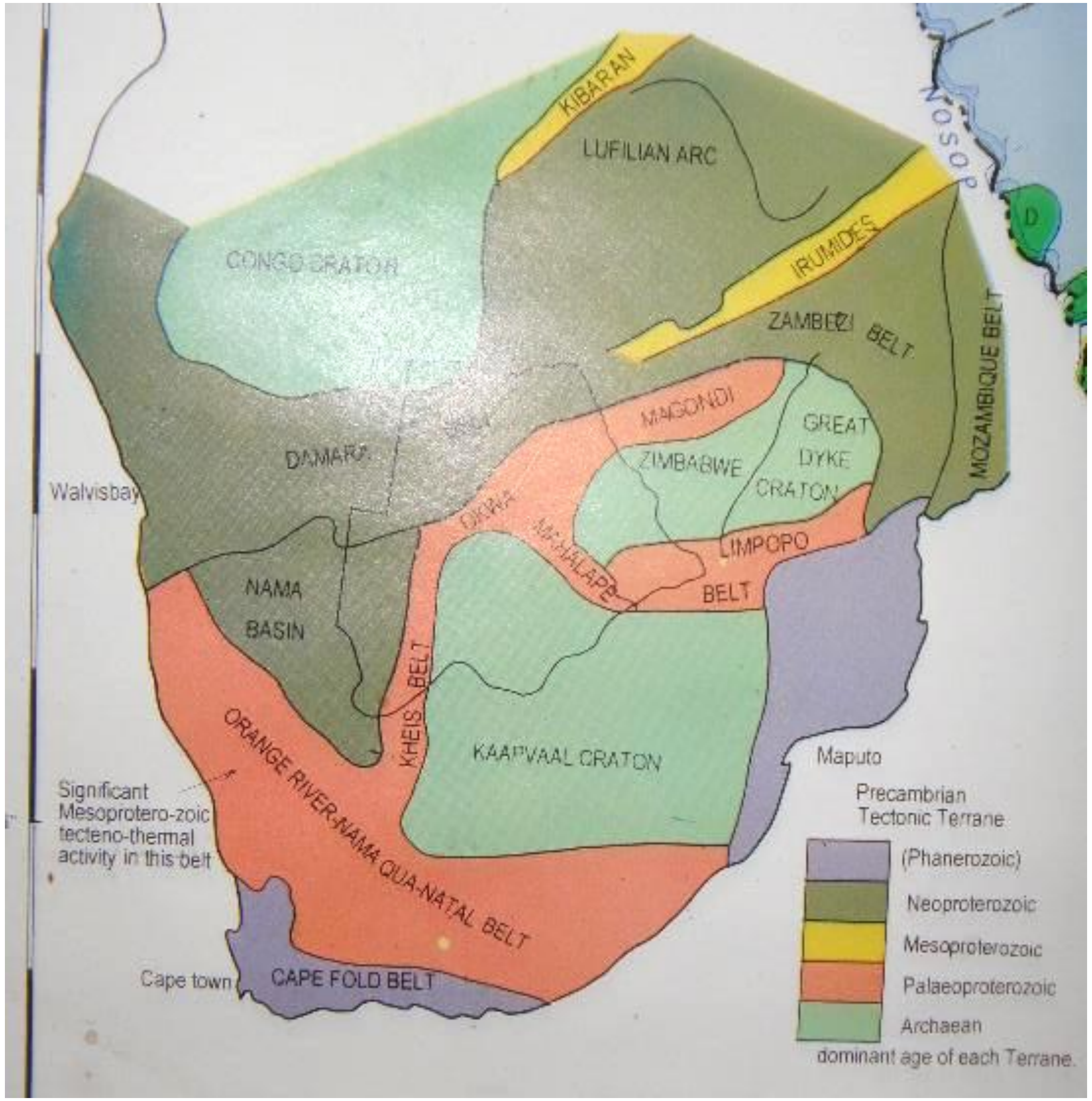


Magondi Belt extends to Botswana

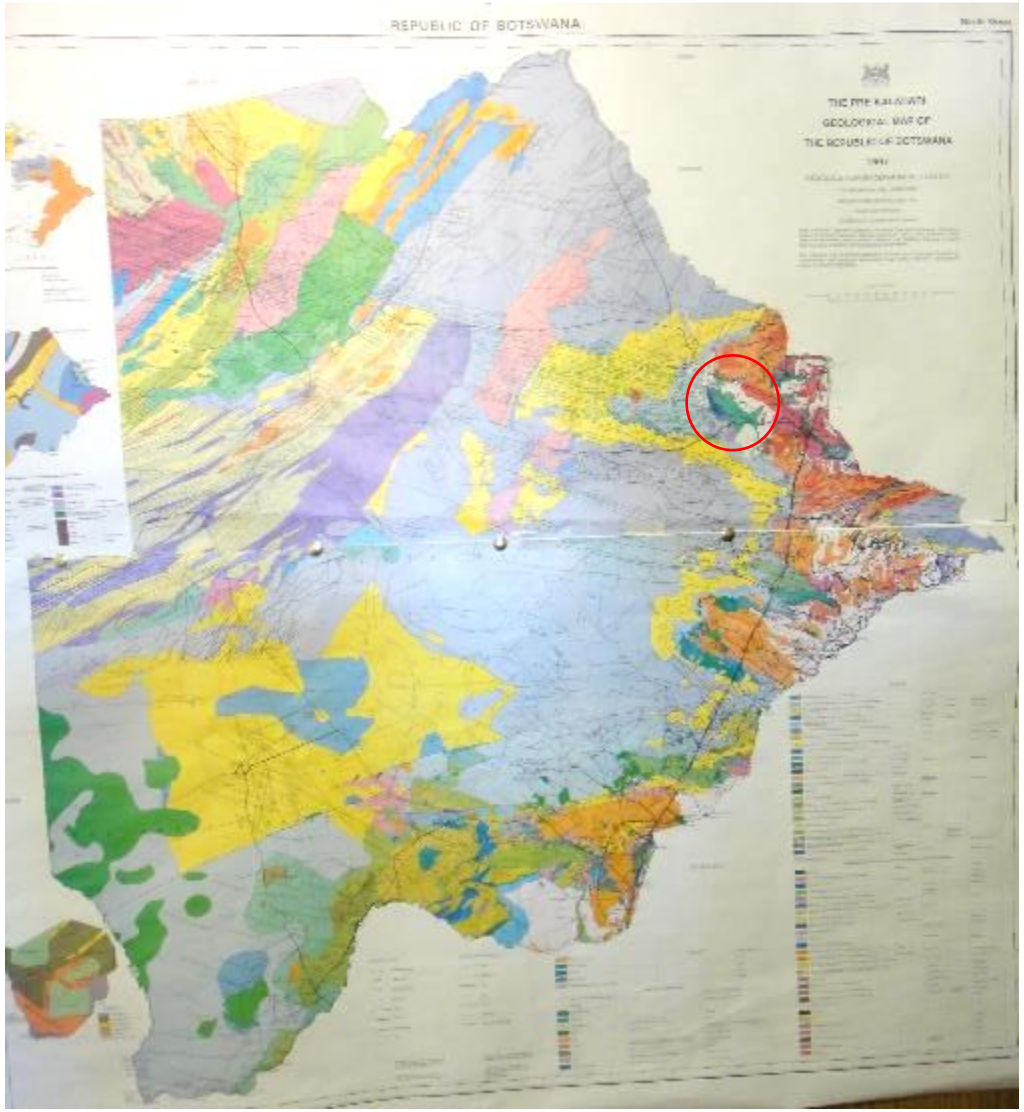


Botswana Subsurface Geology 1:1 million map

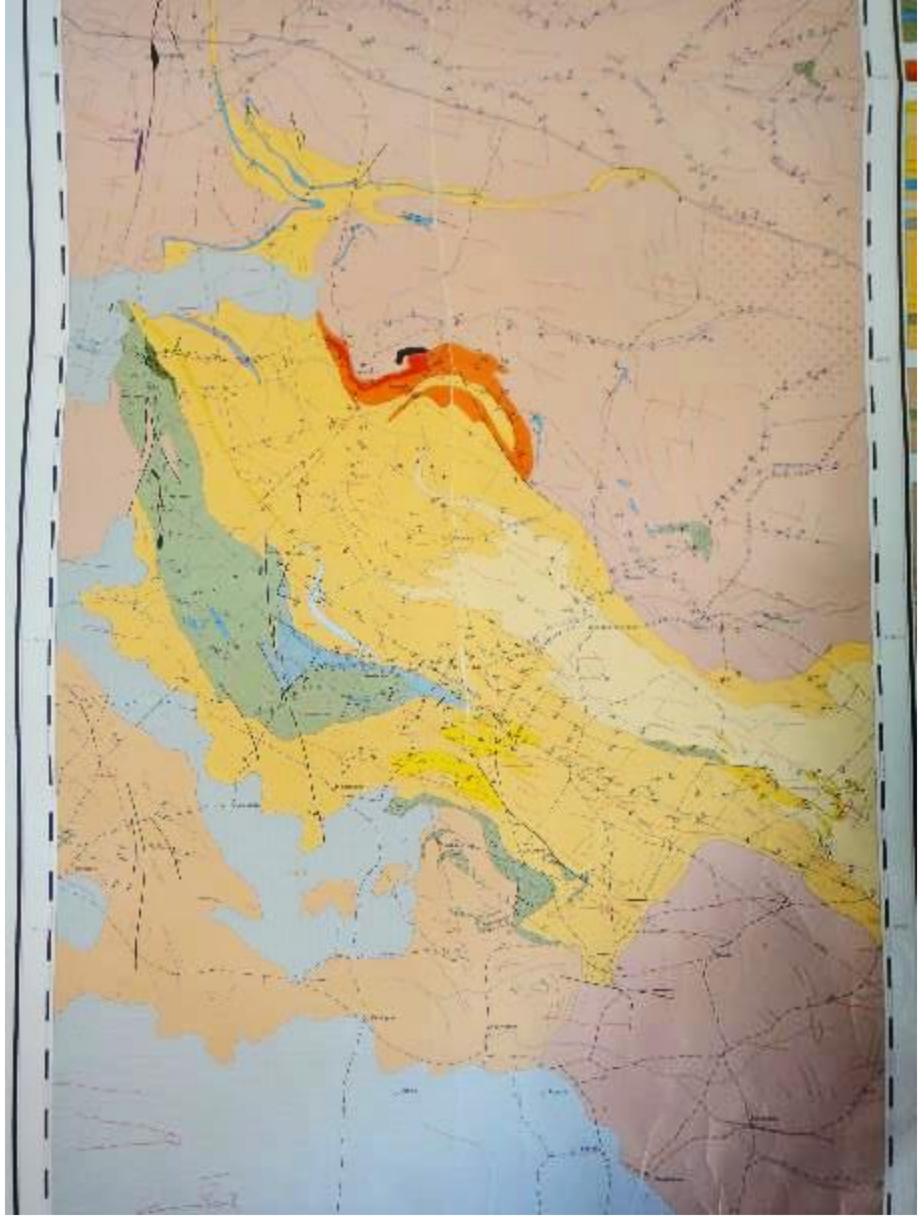

Bennett, J.D., 1970a. Geological map of the Mosetse-Matsitama area (QDS 2026D and 2126B) (1:125 000) with brief explanation. Geological Survey of Botswana.

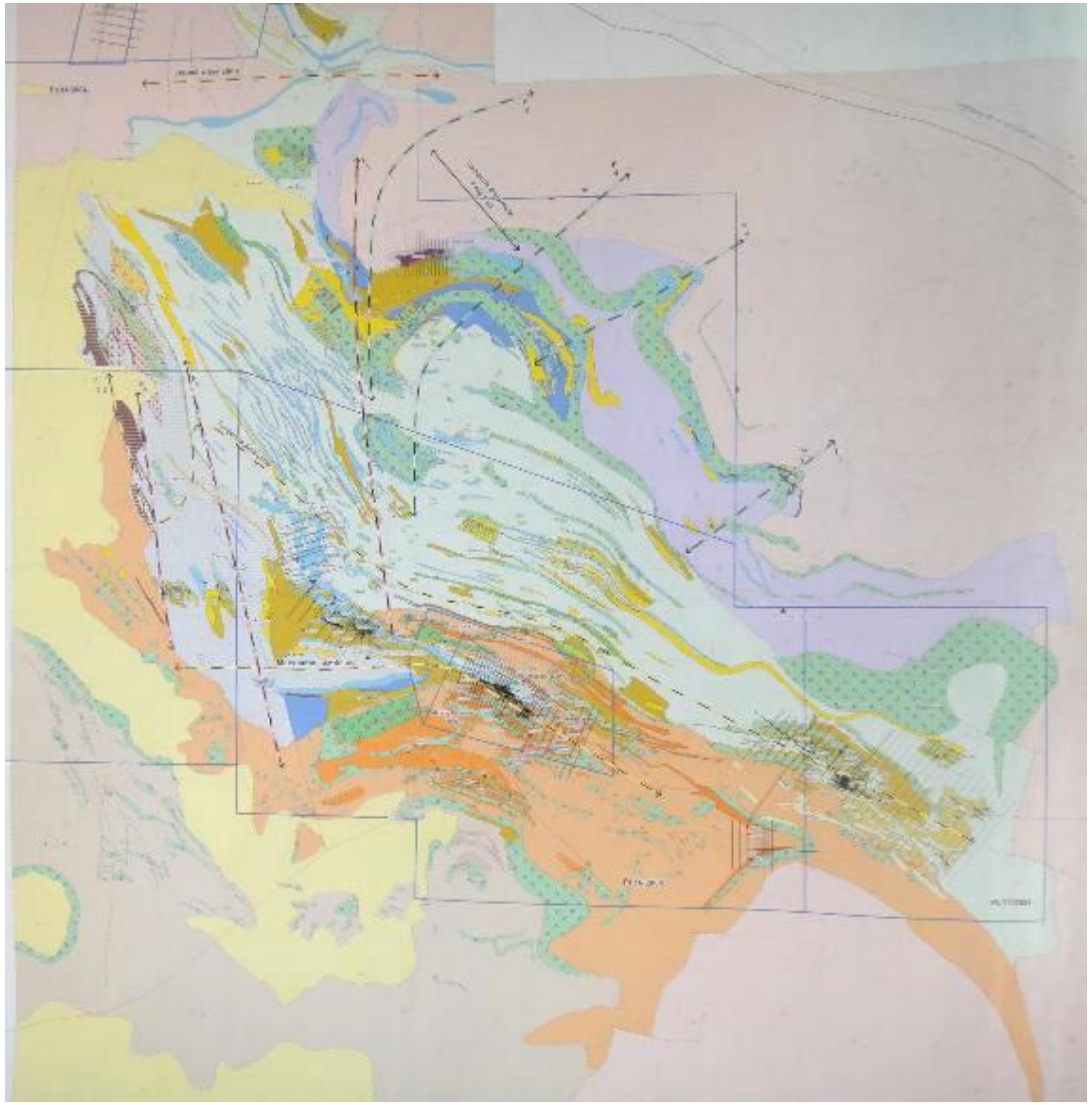

Map of Matsitama Belt (African Copper, 2010)

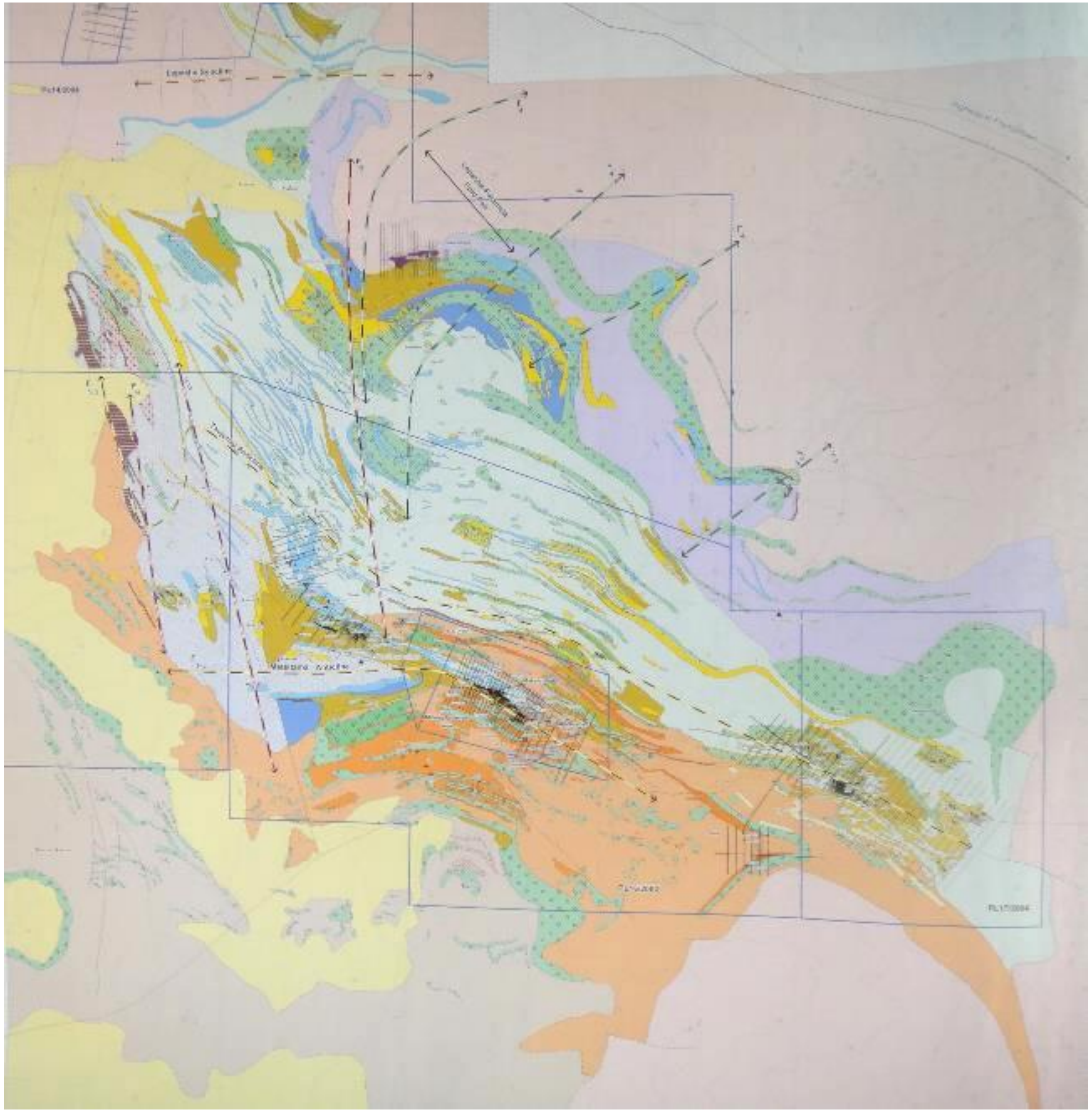

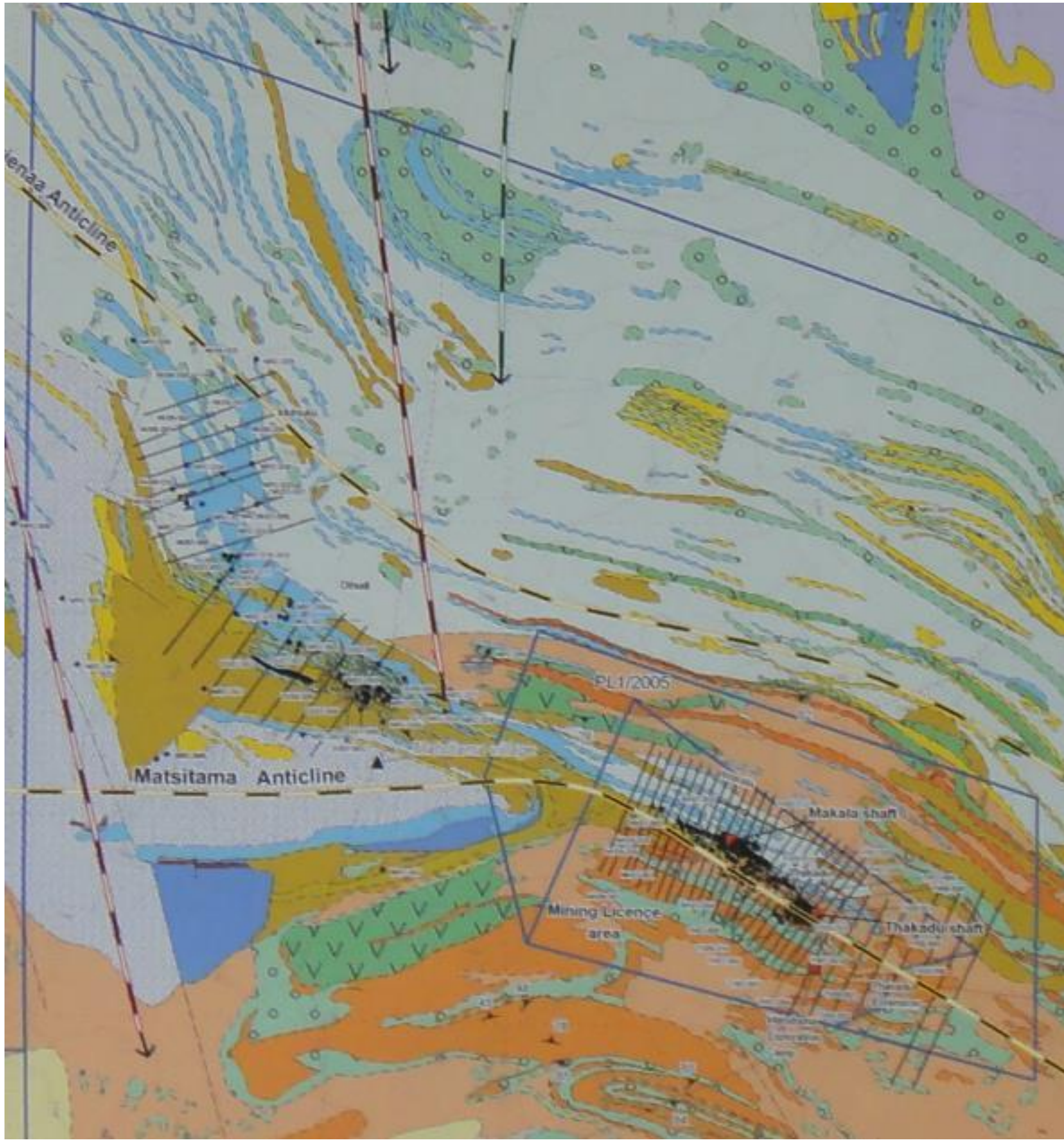


Map of Matsitama Belt (African Copper, 2010)


**High $\delta^{13}C$** Calcite and dolomite marbles ranging up to 9.9 permil $\delta^{13}C$, Matsitama Belt, Botswana, **point to link with the Magondi Belt**, rather than the Archaean Zimbabwe Craton

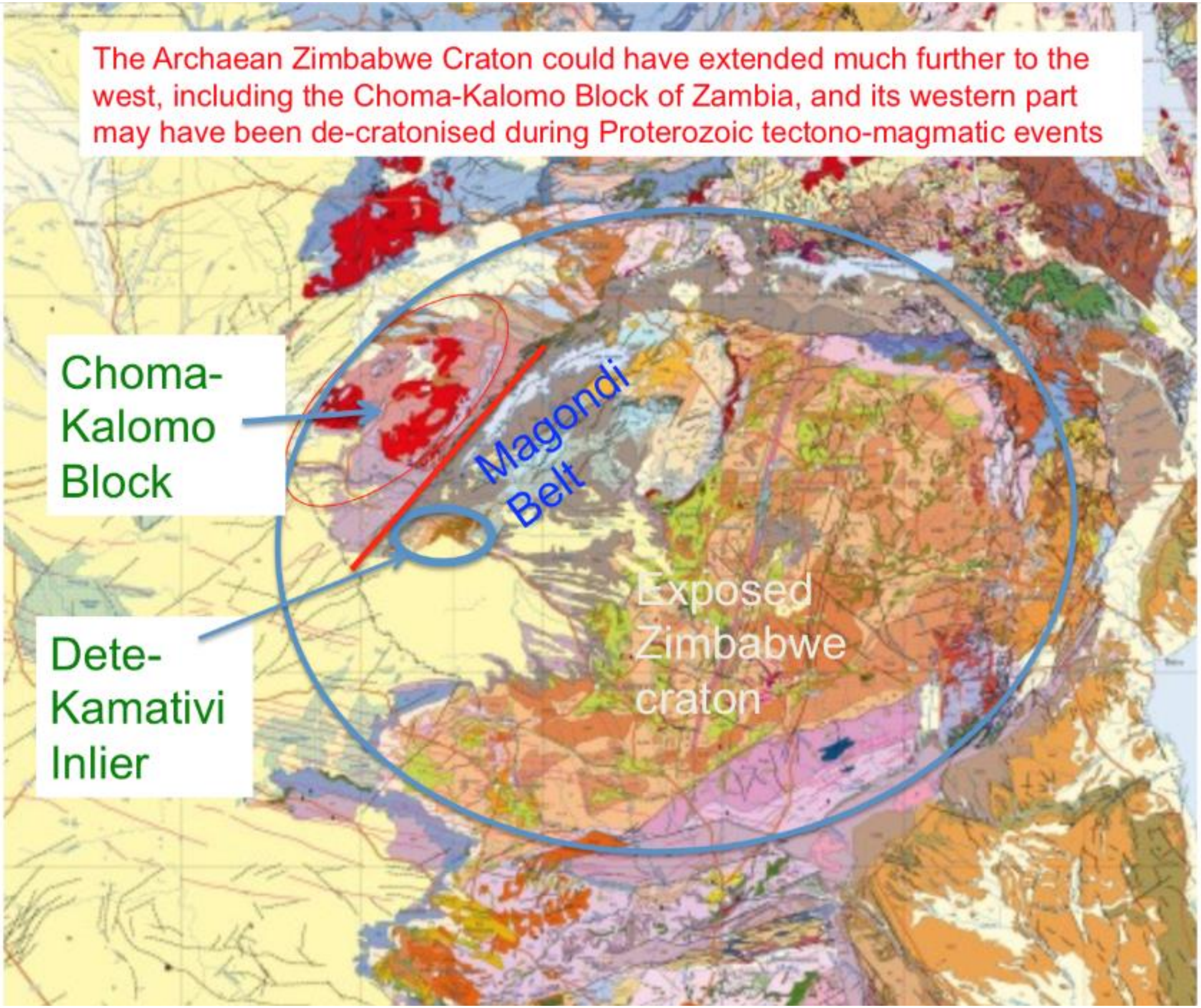
The Archaean Zimbabwe Craton could have extended much further to the west, including the Choma-Kalomo Block of Zambia, and its western part may have been de-cratonised during Proterozoic tectono-magmatic events
Choma-Kalomo Block
Magondi Belt
Dete-Kamativi Inlier
Exposed Zimbabwe craton

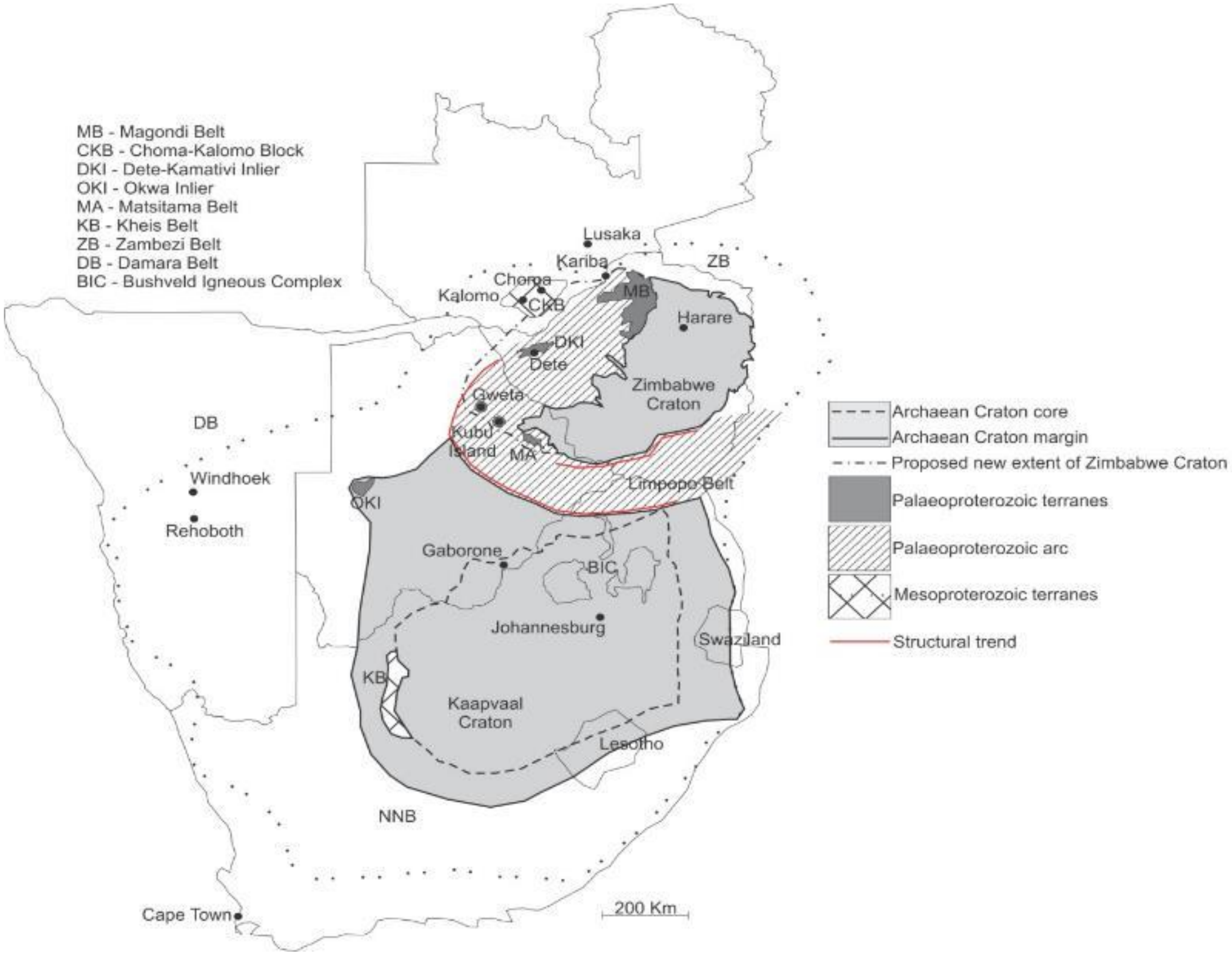

MB - Magondi Belt
CKB - Choma-Kalomo Block
DKI - Dete-Kamativi Inlier
OKI - Okwa Inlier
MA - Matsitama Belt
KB - Kheis Belt
ZB - Zambezi Belt
DB - Damara Belt
BIC - Bushveld Igneous Complex
Lusaka
Kariba
ZB
Choma
Kalomo
CKB
MB
Harare
DKI
Dete
Gweta
Zimbabwe
Craton
Kubu
Island
MA
Limpopo Belt
DB
Windhoek
Rehoboth
OKI
Gaborone
BIC
Johannesburg
Swaziland
KB
Kaapvaal
Craton
Lesotho
NNB
Cape Town
200 Km
Archaean Craton core
Archaean Craton margin
Proposed new extent of Zimbabwe Craton
Palaeoproterozoic terranes
Palaeoproterozoic arc
Mesoproterozoic terranes
Structural trend

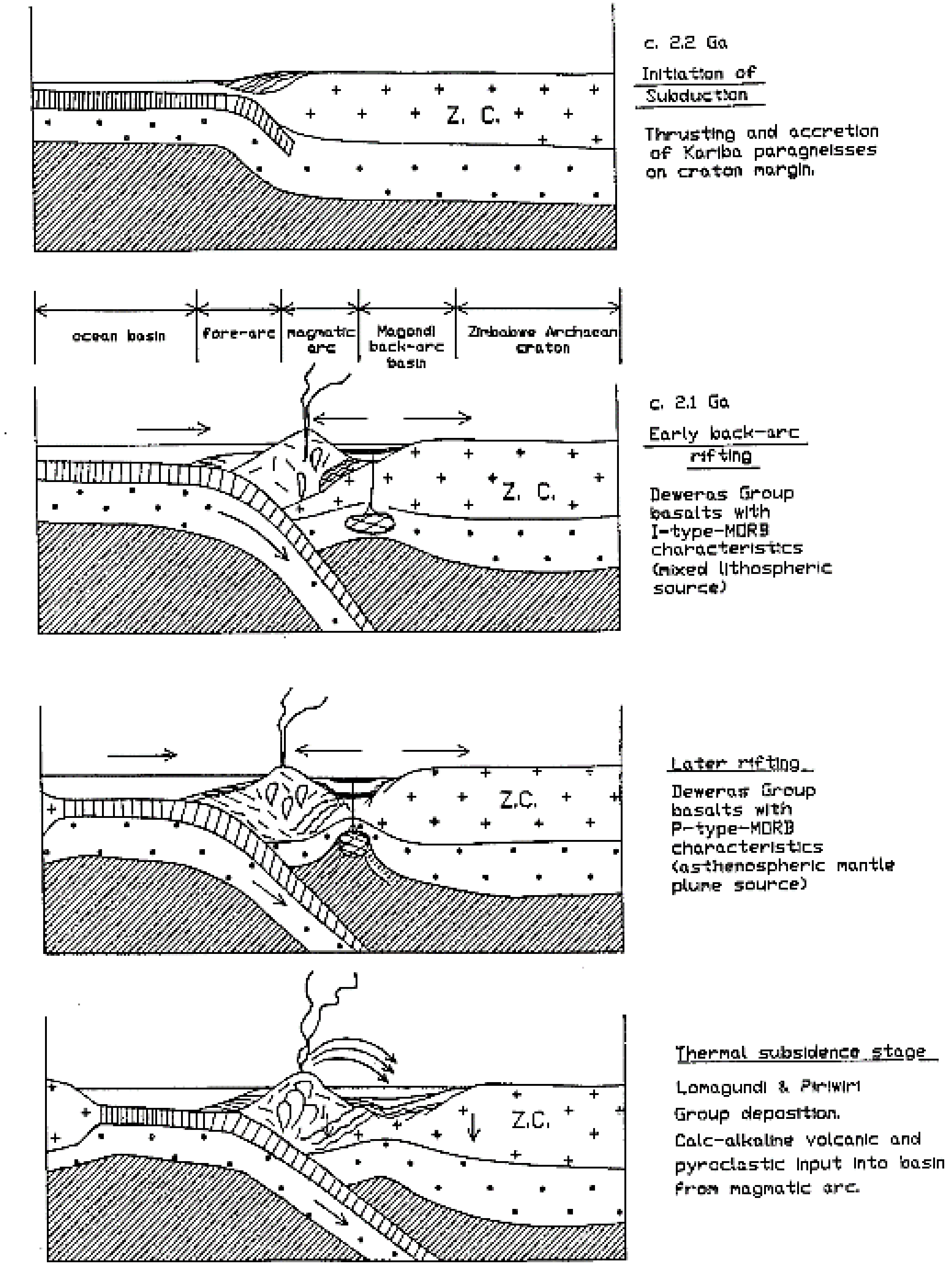


Evolution model for the Magondi belt

Master (1991)

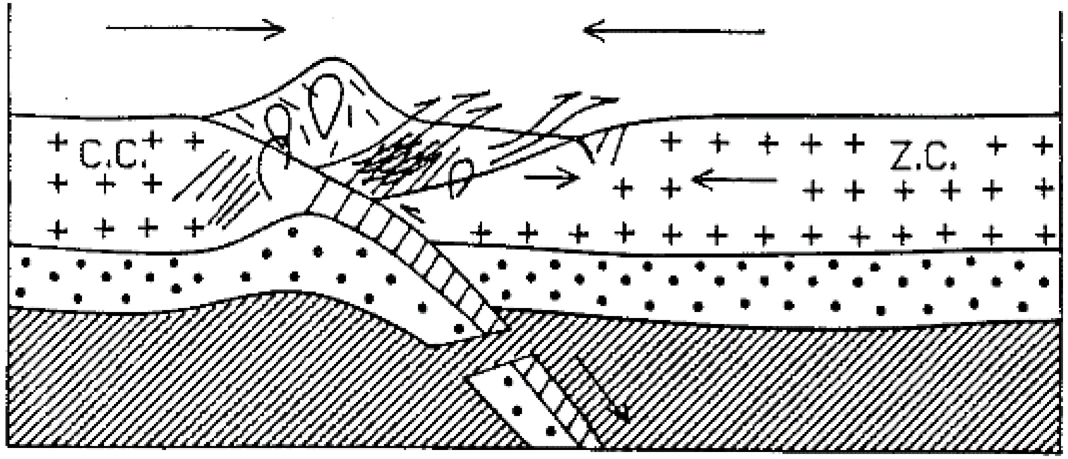


c. 1,8 Ga

Collisional stage

Magondi orogeny.

Magmatic arc thrust over back-arc basin. Back-arc basin sequence thrust onto Zimbabwe craton.

//// = granulite metamorphism

Key.

Continental crust : Z.C. = Zimbabwe craton
C.C. = Congo craton

Juvenile magmatic arc.

Oceanic crust.

Lithospheric mantle.

Juvenile plutons.

Source region for Deweras Group volcanics.

Kariba paragneisses.

Asthenospheric mantle.

# Conclusions I

- The Magondi Supergroup, deposited during the Lomagundi carbon isotope excursion, shows that the perturbations of the carbon cycle affected not only marine rocks (e.g., in the Lomagundi group), but also continental rocks (of the underlying Deweras Group).

# Conclusions II

- The basin developed from continental rift to passive margin (and later to a foreland basin), and in the marine successions there are represented both proximal shallow water and distal deep water facies, and in all facies there are $^{13}C$-enriched carbonate rocks.

# Conclusions III

- Sulphate evaporites are still preserved in the continental facies; relicts of former evaporites occur in the shallow marine facies; black shales, iron and manganese formations, and phosphate beds occur in the deeper marine facies. Furthermore, the metamorphic grade varies along and across the strike of the belt, from prehnite-pumpellyite facies to greenschist, amphibolite and granulite facies.

# Conclusions IV

- All these factors indicate that this basin has the potential to contribute important data concerning the global carbon and sulphur cycles, and the oxidation state of the oceans, during the Lomagundi Event (in both the continental and marine realms, and in shallow and deep water); and it lends itself to the study of the behavior of isotopic systems at different metamorphic grades.

# Our discoveries in the Magondi Belt (1980-2022)- 1.

- **Sulphate evaporite beds** (anhydrite, partly replaced by barite) and gypsum and anhydrite veins at Norah Mine.
- **Aeolianites** in the Deweras Group- the oldest desert
- **Geochronological framework** for Magondi Belt
- **Andean-type magmatic arc** in the western Magondi Belt

# Our discoveries in the Magondi Belt (1980-2022)- 2.

- Proof that the **Mangula Granite is part of the Archaean basement**, and is NOT intrusive into the Deweras Rocks at Mhangura.
- Detailed studies (including ore mineral zonation, contact metamorphism by early mafic sills, relation to faults, permeable zones, and reduced beds) proving the **early diagenetic origin of stratabound sediment-hosted Cu-Ag mineralization** in the Deweras Group
- Detailed mapping showing the **origin of quartz-carbonate veins** in the mafic sill at Norah originating from pressure-solution in semipelitic mineralized wallrocks during the Magondi Orogeny
- Detailed studies using metamorphic textures such as syntectonic replacement of pyrite by chalcocite or djurleite, showing **syntectonic origin of mineralization in Lomagundi Dolomites** at Alaska and Cedric Mines.

# Our discoveries in the Magondi Belt (1980-2022)- 3.

- Geochronological studies supporting the lithostratigraphic correlation of the protoliths of the Dete-Kamativi Inlier with the main Magondi Supergroup.
- Discovery of the **Lomagundi Carbon Isotope Anomaly** (LCIA) also in the **continental rocks of the Deweras Group,** showing that it was due to a perturbation of the entire Carbon Cycle, and not just in the oceans.
- Discovery of the **LCIA in carbonate rocks of the Matsitama Belt** in eastern Botswana, proving that the belt is composite, and contains a Magondian component thrust onto an older Archaean greenstone belt, thus explaining the anomalously young Pb ages, and the presence of redbeds in that belt.
- Detailed analysis of the tectonosedimentary setting of the **Magondi Belt** leading to the interpretation of its tectonic setting as being deposited in a **continental back-arc basin**, behind an Andean-type magmatic arc.
- Considerations based on the age and correlations of dykes leading to the conclusion that the Zimbabwe Craton was attached to the eastern end of the Superior Craton, adjacent to the Labrador Trough, before rifting away at around 2.1 Ga and colliding with the Kaapvaal Craton

Master et al., 2010, Prec. Res.

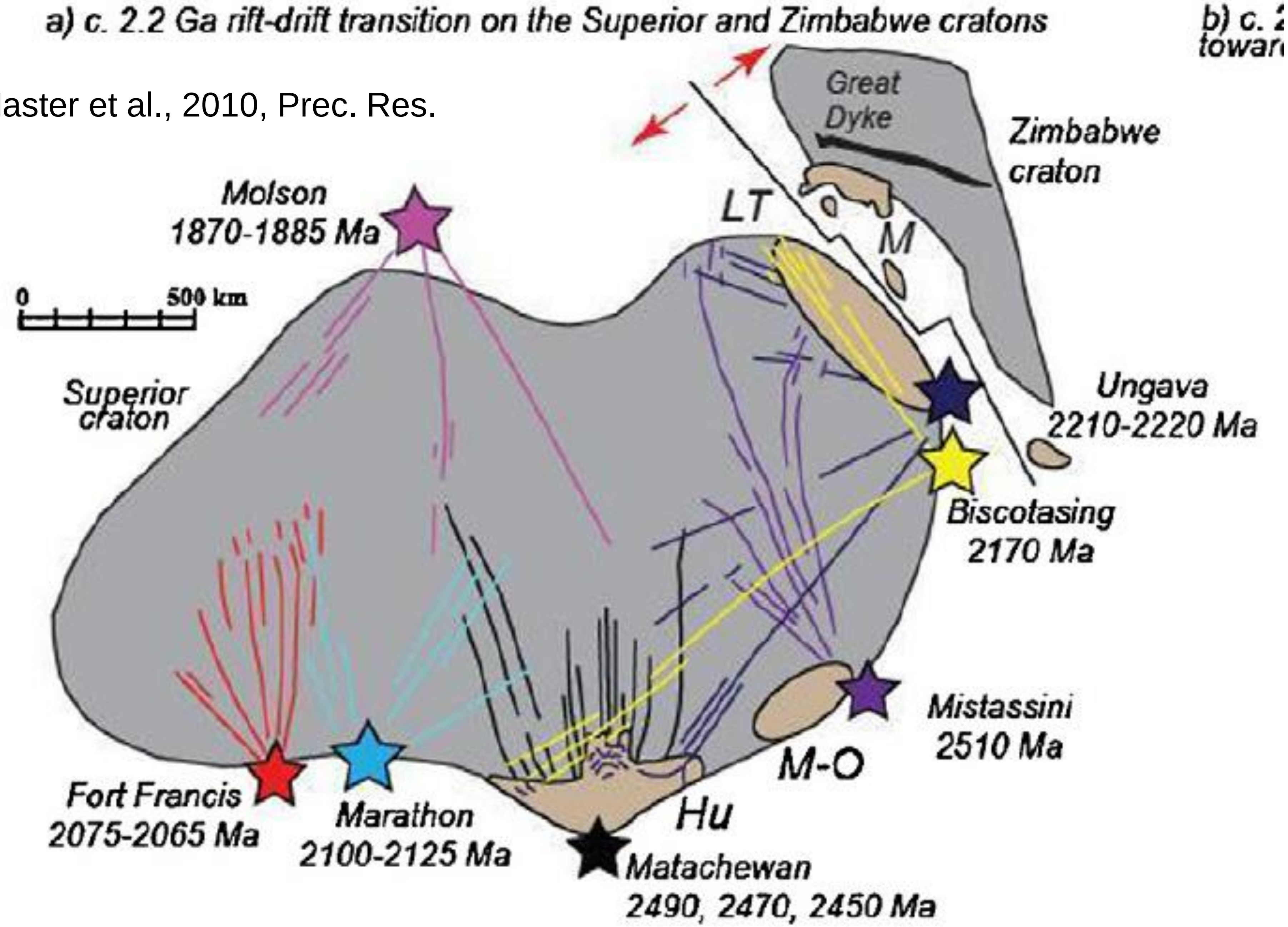

b) c. 2.1 Ga oblique collision of the Kaapvaal craton and unknown terrane, rotation towards the Zimbabwe craton with subduction zones and back-arc basin developed

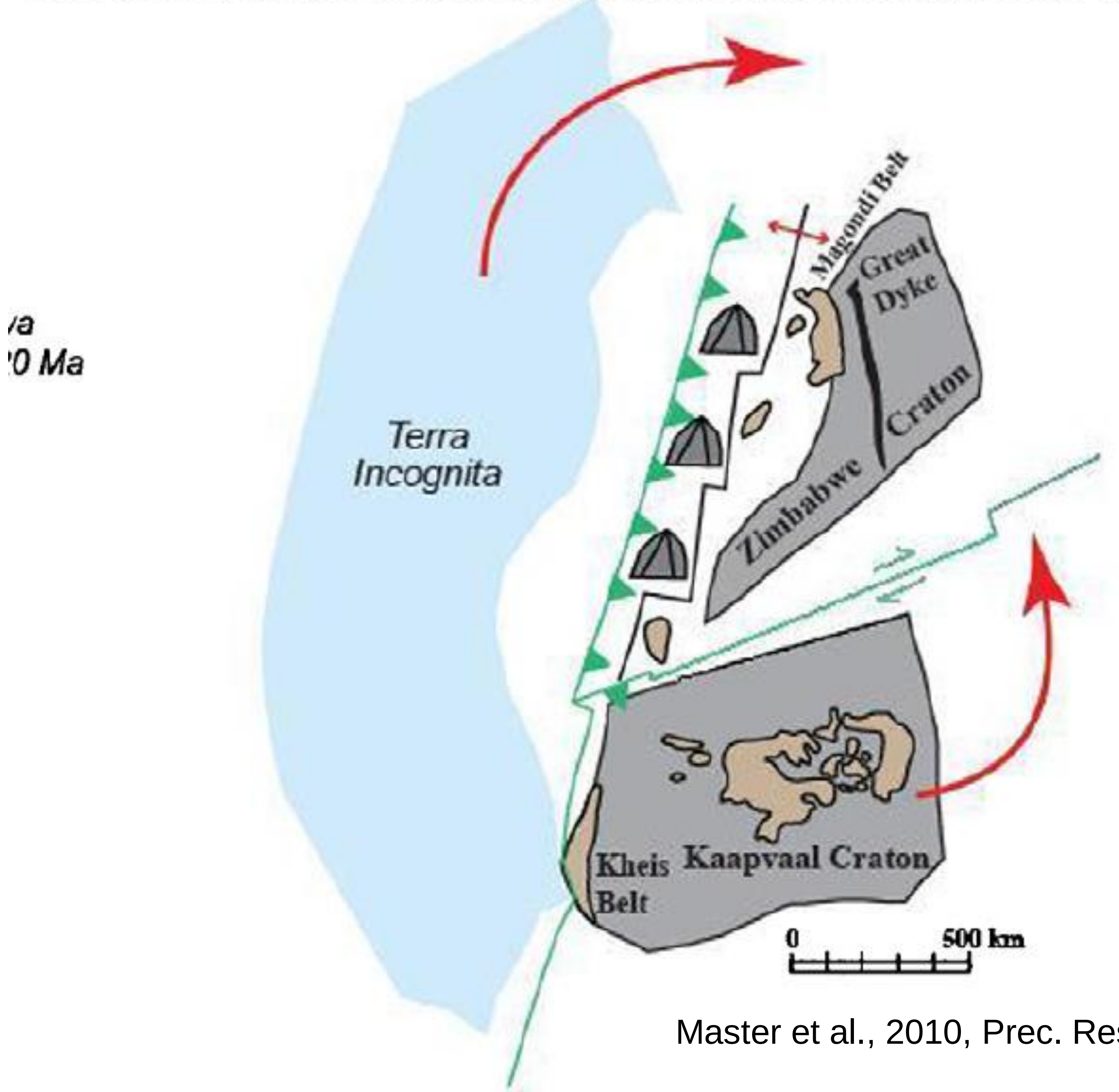


Master et al., 2010, Prec. Res.

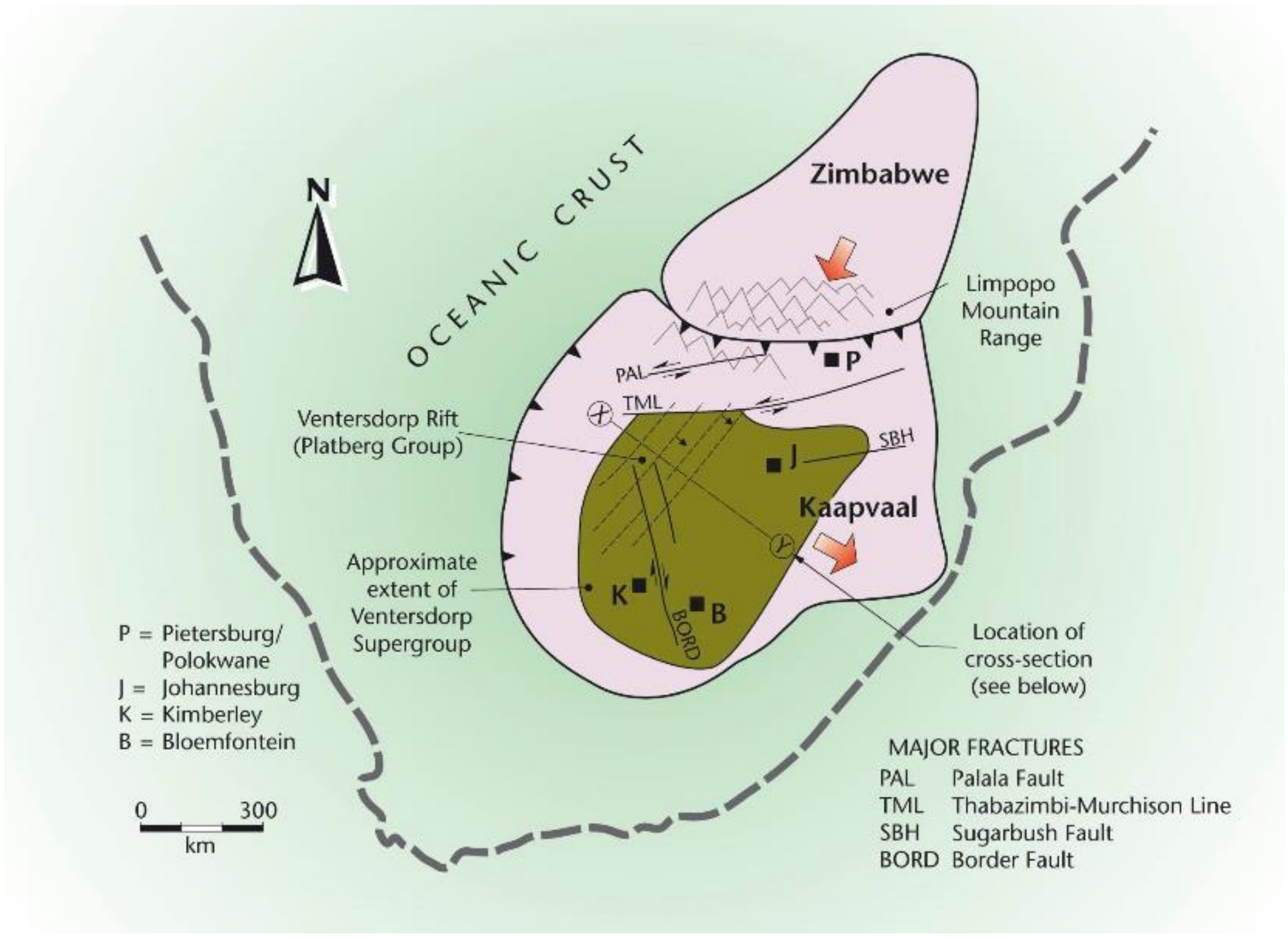


McCarthy & Rubidge 2004

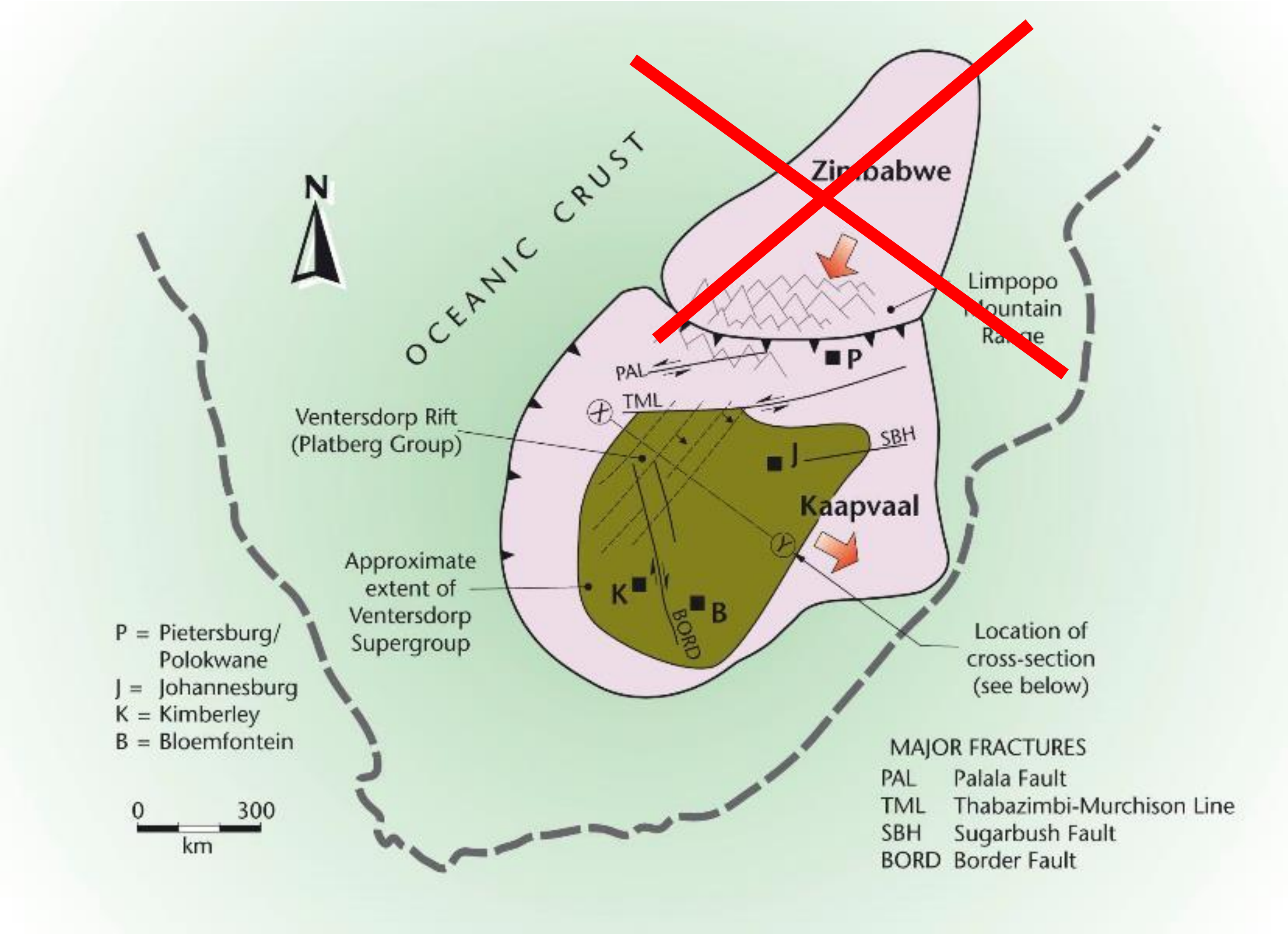
N
OCEANIC CRUST
Zimbabwe
Limpopo Mountain Range
P
PAL
TML
SBH
J
Kaapvaal
K
B
BORD
Ventersdorp Rift (Platberg Group)
Approximate extent of Ventersdorp Supergroup
Location of cross-section (see below)
P = Pietersburg/ Polokwane
J = Johannesburg
K = Kimberley
B = Bloemfontein
0 300
km
MAJOR FRACTURES
PAL Palala Fault
TML Thabazimbi-Murchison Line
SBH Sugarbush Fault
BORD Border Fault

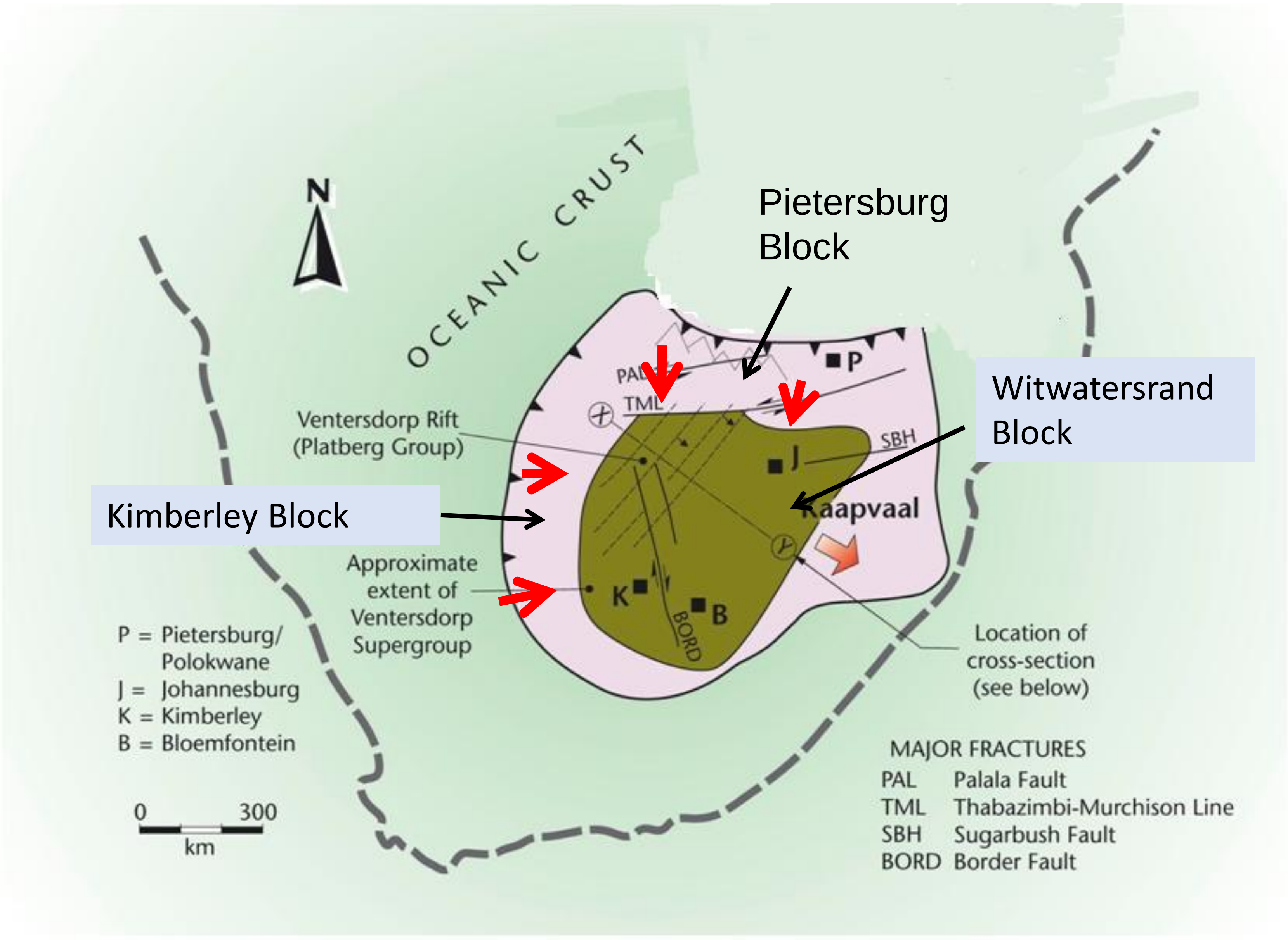
N
OCEANIC CRUST
Pietersburg Block
Witwatersrand Block
Kimberley Block
PAL
TML
P
SBH
J
Kaapvaal
K
B
BORD
Ventersdorp Rift (Platberg Group)
Approximate extent of Ventersdorp Supergroup
Location of cross-section (see below)
P = Pietersburg/ Polokwane
J = Johannesburg
K = Kimberley
B = Bloemfontein
0 300 km
MAJOR FRACTURES
PAL Palala Fault
TML Thabazimbi-Murchison Line
SBH Sugarbush Fault
BORD Border Fault

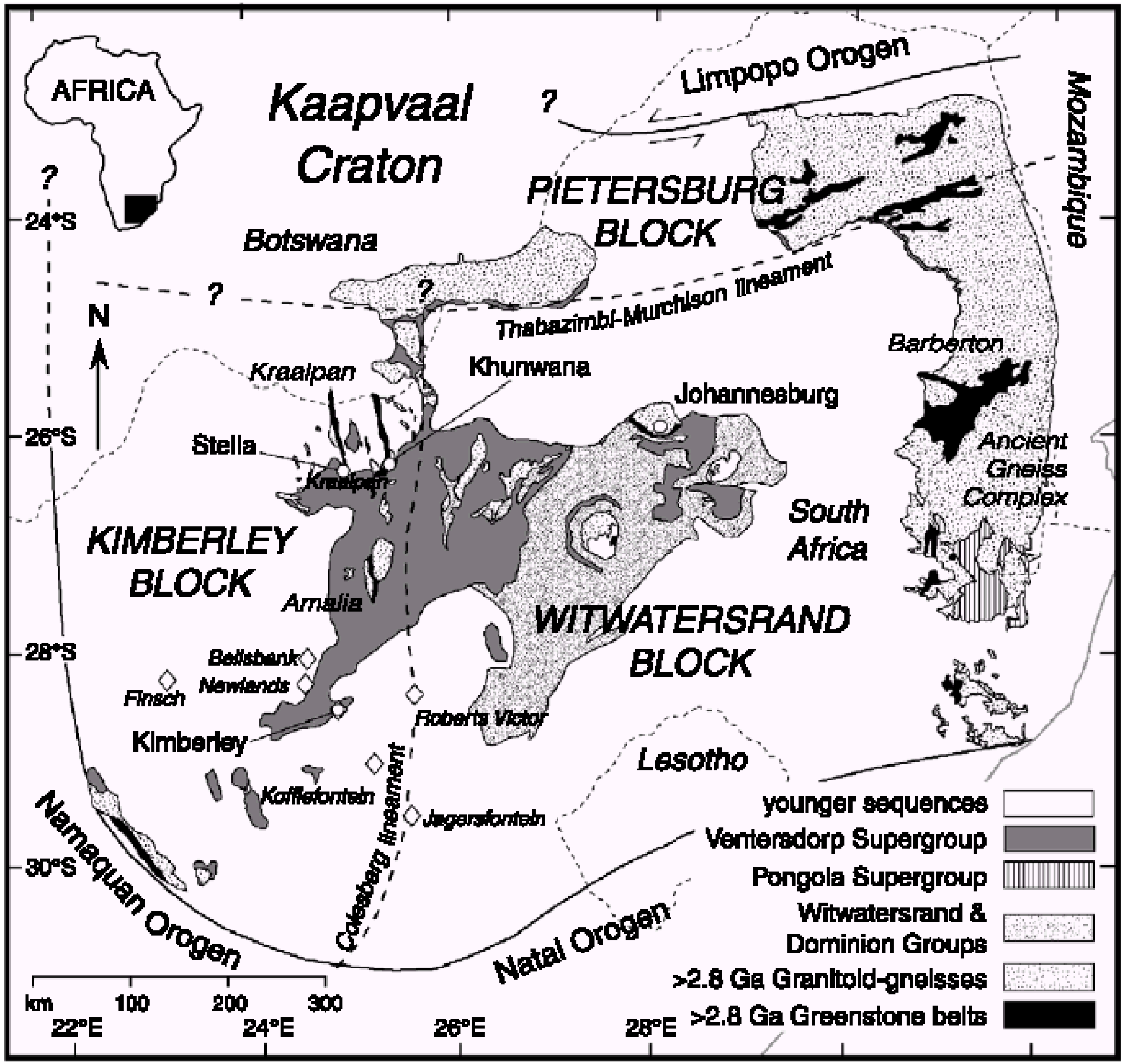

AFRICA
Kaapvaal Craton
Limpopo Orogen
Mozambique
PIETERSBURG BLOCK
Botswana
Thabazimbi-Murchison lineament
Barberton
Kraaipan
Khunwana
Johannesburg
Stella
Ancient Gneiss Complex
South Africa
KIMBERLEY BLOCK
Amalia
WITWATERSRAND BLOCK
Bellsbank
Newlands
Finsch
Roberts Victor
Kimberley
Lesotho
Koffiefontein
Colesberg lineament
Jagersfontein
Namaquan Orogen
Natal Orogen
younger sequences
Ventersdorp Supergroup
Pongola Supergroup
Witwatersrand & Dominion Groups
>2.8 Ga Granitoid-gneisses
>2.8 Ga Greenstone belts
km 100 200 300
24°S
26°S
28°S
30°S
22°E
24°E
26°E
28°E
N

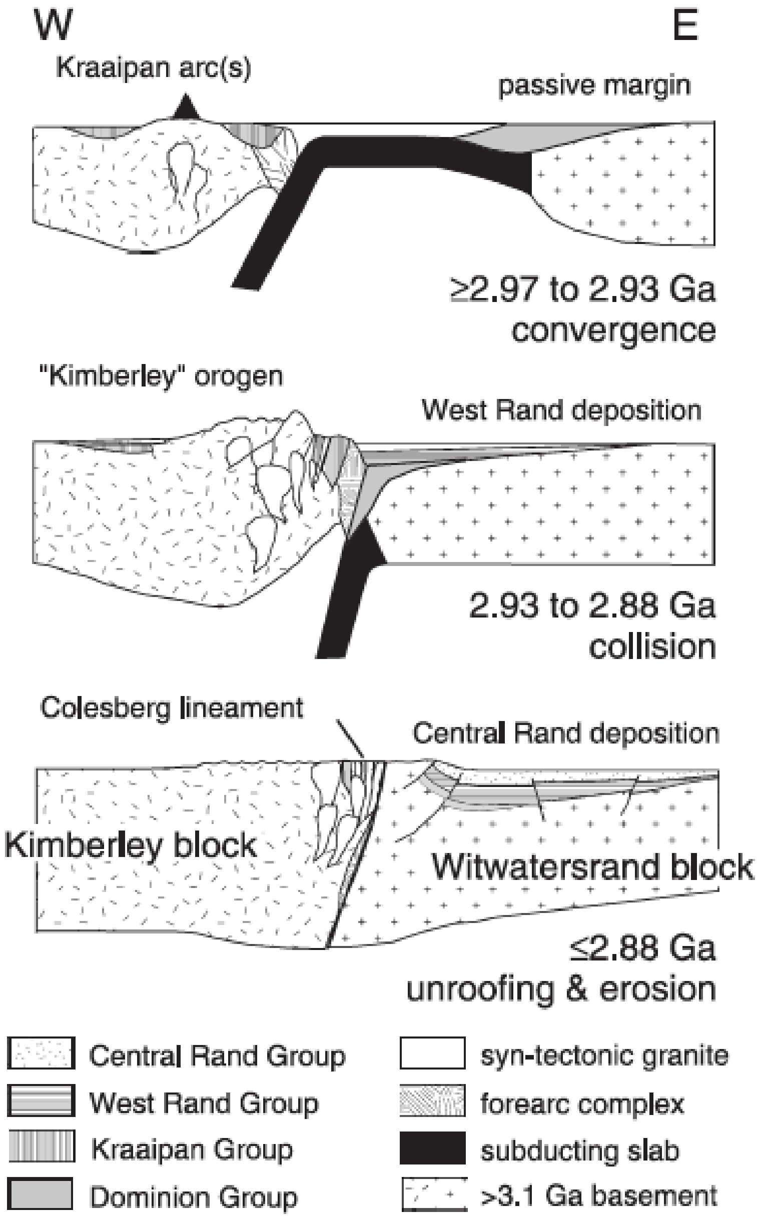


Fig. 4. Schematic E–W cross-sections through the Kimberley and Witwatersrand blocks. The sequence of sections illustrate the inferred model of ca. 2.9 Ga west-dipping (present-day geography) subduction-convergence and collisional suturing.

# **Foreland Basin model for the Witwatersrand Basin**, during collision of the Kimberley block with the Witwatersrand block

Schmitz et al. (2004), EPSL, 222, 363-376.

# Acknowledgements

- I would like to express my sincere thanks to the Geological Society of Zimbabwe, through its then Secretary Kudzai Musiwa, for inviting me to give this lecture.
- I owe a great debt of gratitude to all my mentors, colleagues and collaborators who guided my career in geology from the very earliest days, when I started working as a mine geologist in Zimbabwe in 1980. Some of the people who influenced me in this country were ”Bish” Bichard, Tim Broderick, Tony Martin, Dave Bartholomew, Henry Simpson, Jan Kramers, Tom Blenkinsop, Hubert Munyanyiwa, and Jimmy Wilson.
- I am very grateful to Jane and Andrew du Toit for hosting me in Harare, and to Fiona and Martin Rowe for hosting me in Bulawayo.
- Thanks to Andrew du Toit for organizing the field excursion

# Thank you!